REPUBLIC OF TURKEY
BİNGÖL UNIVERSITY
INSTITUTE OF SCIENCE

THE EFFECT OF DEPOSITION TIME ON PERFORMANCE OF Cu_2O PHOTOELECTRODES PREPARED BY THE ELECTROCHEMICAL METHOD

MASTER'S THESIS

SHIVAN JAWHAR TAHER

CHEMISTRY

THESIS ADVISOR
Prof. Dr. İBRAHİM Y. ERDOĞAN

BİNGÖL-2017

REPUBLIC OF TURKEY
BİNGÖL UNIVERSITY
INSTITUTE OF SCIENCE

THE EFFECT OF DEPOSITION TIME ON PERFORMANCE OF Cu_2O PHOTOELECTRODES PREPARED BY THE ELECTROCHEMICAL METHOD

MASTER'S THESIS

Shivan Jawhar TAHER

Department : CHEMİSTRY

This dissertation was accepted by the following committee on 17.08.2017 with the vote unity.

Prof. Dr.	**Prof. Dr.**	**Prof. Dr.**
Latif KELEBEKLİ	**Ramazan SOLMAZ**	**İbrahim Y. ERDOĞAN**
Head of examining committee	**Member of examining committee**	**Member of examining committee**

I confirm the result above

Prof. Dr. İbrahim Y. ERDOĞAN

Director of the institute

PREFACE

The first of all, I want to express my best thanks to merciful Allah who have been given me enough strength to perform and complete my scientific project successfully.

A special gratitude to my supervisor Prof. Dr. İbrahim Y. ERDOĞAN, a true guide who supported and encouraged me during the entire tenure of the project. He inspired me to drive this thesis towards the path of glory and success.

I would like to express my deepest appreciation to Chemistry Department and Central Laboratory staff and to all those who provide me the possibility to complete this research.

Finally, special thanks to my mom (Nasreen), my brothers (Karzan, Alan) my sister (Zhwan), wife (Munira), son (Muhammad) and daughter (Haneen), and all my friends for their help.

Shivan Jawhar Taher

Bingöl 2017

CONTENTS

LIST OF SYMBOLS AND ABBREVIATIONS

A	: Ampere
cm^2	: Centimeters meter square
CV	: Cyclic voltammetry
d	: Distance
E	: Electrode potential
E	: Standard electrode potential
ED	: Electrodeposition
Eg	: Energy band
eV	: Electron volts
FETs	: Field-effect transistors
g	: Gram
Ipa	: Anodic peak current
Ipc	: Cathodic peak current
K	: Kelvin
kj	: Kilojoule
L	: Litter
Log	: Logarithm
mA	: Miliampere
mAh	: Miliamper-hour
mm	: Milimeter
mL	: Mililitter
mV	: Milivolt
μm	: Micrometer
n	: Number of electrons
nm	: Nanometer
Pa	: Pascal

PEC	: Photoelectrochemistry
s	: Second
Sccm	: Standard cubic centimeter-minute
T	: Temperature
t	: Time
UPD	: Underpotential deposition
V	: Volt
Ω	: Electrical resistance
λ	: Wavelength

LIST OF FIGURES

ELEKTROKİMYASAL YÖNTEMLE HAZIRLANAN Cu_2O FOTOELEKTROTLARIN PERFORMANSINA DEPOZİSYON ZAMANININ ETKİSİ

ÖZET

Bu tez çalışması, Cu_2O yarıiletken fotoelektrotların fotoelektrokimyasal özelliklerine elektrodepozisyon zamanının etkisi üzerine sistematik bir çalışmadır. Bakır (I) oksit fotoelektrotları potansiyelaltı depozisyon (UPD) temelli elektrokimyasal yöntem kullanılarak hazırlandı. Cu_2O yarıiletken fotoelektrotların karakterizasyonu X-ışını kırınımı (XRD), taramalı elektron mikroskopu (SEM), enerji dağılımlı X-ışını spektroskopisi (EDX), morötesi-görünür bölge (UV-Vis) spektroskopisi, doğrusal taramalı voltametri (LSV) ve kronoamperometri (CA) teknikleri kullanılarak gerçekleştirildi. XRD sonuçları ITO substrat üzerine biriktirilen Cu_2O yarıiletkenlerinin yüksek kristal yapıya sahip olduğunu gösterir. SEM görüntüleri küp biçimli Cu_2O kristallerinden oluşan bir morfoloji gösterdi. EDX ve optiksel band gap sonuçları tüm örnekler için tek faz Cu_2O varlığını doğrular. Bu çalışma, 15 dakika elektrodepozisyonla hazırlanan Cu_2O yarıiletken fotoelektrotların incelenen tüm elektrotlar arasında en yüksek fotoakım ve akım yoğunluğu sergilediğini gösterdi. Tüm elektrokimyasal ölçümler, Cu_2O yarıiletkenlerinin p-tipi doğasına bağlı olarak fotokatodik davranış gösterdi. Cu_2O fotoelektrotlar farklı depozisyon zamanları için iyi bir kararlılık davranışı sergiledi. Cu_2O yarıiletken fotoelektrotları, ileri fotoelektrokimyasal dedeksiyon, fotoelektrokimya su ayrıştırma ve diğer solar fotovoltaik teknolojilerin geniş bir alanı için rekabetçi bir aday olarak önerilebilir.

Anahtar Kelimeler: Bakır (I) oksit, elektrokimyasal depozisyon, depozisyon zamanı, fotoelektrokimya.

THE EFFECT OF DEPOSİTİON TIME ON PERFORMANCE OF Cu_2O PHOTOELECTRODES PREPARED BY THE ELECTROCHEMICAL METHOD

ABSTRACT

This thesis study reports on a systematic study of the influence of the electrodeposition time on the photoelectrochemical characteristics of Cu_2O semiconductors photoelectrodes. Copper (I) oxides photoelectrodes were prepared by the electrochemical method, based on the underpotential deposition (UPD). The characterization of Cu_2O semiconductors photoelectrodes was performed by X-ray diffraction (XRD), scanning electron microscopy (SEM), energy dispersive X-ray spectroscopy (EDX), ultraviolet–visible (UV–Vis) spectroscopy, linear sweep voltammerry (LSV) and chronoamperometry (CA) techniques. XRD results indicate that Cu_2O semiconductors deposited over ITO substrate have highly crystalline structure. SEM images showed a morphology with cube-shaped Cu_2O. EDX and the optical band gap results confirm the presence of single phase Cu_2O for all the samples. This work showed that the Cu_2O semiconductor photoelectrodes electrodeposited for 15 min exhibit the highest photocurrents and the current density between the investigated all semiconductor films. All the electrochemical measurements showed a photocathodic behavior due to the p-type nature of the Cu_2O semiconductors. Cu_2O photoelectrodes exhibited a good stability behavior for different Cu_2O electrodeposition times. Cu_2O semiconductor photoelectrodes are suggested as a competitive candidate for advanced photoelectrochemical detection, maybe for the extended field of photoelectrochemical water splitting and other solar photovoltaic technologies.

Keywords: Copper (I) oxide, electrochemical deposition, deposition time, photoelectrochemistry.

1. INTRODUCTION

Photoelectrochemistry is a branch of chemistry that is deals with the study within electrochemistry concerned with the interaction of light with electrochemical systems. It is an active field of investigation. One of the developers of this field of electrochemistry was the German electrochemist Heinz Gerischer. The interest in this field is high in the context of development of renewable energy conversion and storage technology (Parkinson et al.1978).

Photoelectrochemical cells are solar cells that are changed light source into an electrical energy; in this process we can obtain electrical energy including the visible region. Each cell involves a photocathode and a metal anodal immersed in a semiconducting electrolyte. The basis of solar cell systems is the semiconductor technology, which has a very important place for energy production at this time. The major properties of semiconductor material make them useful as essential elements in electronic circuits. A photoelectrochemical process takes three steps. In the first step, an electronic charge is formed on the surface of the photocathode sensitive to the sun's rays, creating electron hole pairs. In the second step, electrons and protons in the photocathode are reduced to hydrogen molecules. In the third step, the conduction of the photocathodically anodic holes is through electrolytic and electrical connection is mentioned. The properties of semiconductor materials that are forming the photoelectrodes play an important role in the solar energy conversion efficiency (Sze et al.2007).

Photoelectrochemical measurement is actually sensitive as electrochemiluminescence due to the complete the separation of excitation light source and finding photocurrent signal, it is lately developed and promising analytical technique the utilization of electronic detection makes the photoelectrochemical instruments low cost and simpler. The sensitive photoelectrochemical determination based on excellent photoelectric light with the higher response of photo and promoted photoelectric conversion efficiency. Most of the photoelectrochemical designs are relying on heterojunction of semiconductor, and

surface Plasmon resonance for noble metal, between the above methods, the properties of the semiconductor heterojunction dominate the behavior of photo-induced charge carriers, such as the transport direction, the separation distance, and the recombination rate (Li et al. 2014).

Semiconductors are crystalline or amorphous solids with different electrical characteristics. They are of high electrical resistance higher than typical resistance of materials, but still of very lower resistance than insulators. Their resistance decreases by increasing in their temperature, which is behavior opposite to that of a metal. Finally, their conducting characteristics may be altered in useful ways by the deliberate, controlled introduction of impurities into the crystal structure, which decrease its resistance but also permits the creation of semiconductor junctions between differently-doped regions of the extrinsic semiconductor crystal. The action of charge carriers which include electrons, electron holes and ions at these junctions is the basis of transistors, diodes and all modern electronics (Mehta 2008).

Semiconductor devices has a range of useful properties such as current passing more easily in one direction than the other, displaying inconstant resistance, and sensitivity to heat or light. Because the electrical properties of a semiconductor material can be doping modify, or by the application of electrical or light fields, devices made from semiconductors can be used for switching, amplification, and energy conversion. The modern accepting of the properties of a semiconductor relies on quantum physics to explain the movement of charge carriers in a crystal lattice. Doping really increases the number of charge carriers with in the crystal. When a doped semiconductor contains mostly free holes it is called "p-type", and when it contains mostly free electrons it is named as" n-type". The semiconductor materials used in electronic devices are doped under precise conditions to control the concentration and regions of p-type and n-type dopants. The single semiconductor crystal can have several p-type and n-type regions; the p–n junctions between these regions are in charge for the useful electronic behavior (Turley and Jim 2002).

The semiconductors are widely used in electronic technology, with the most important respects being the integrated circuit. Some devices contain integrated circuits; cell-

phones, laptops, scanners, etc. Semiconductors for integrated circuits are mass-produced. To produce an ideal semiconducting material, chemical purity is very important. Any small deficiency can have a radical effect on how the semiconducting material behaves due to the scale at which the materials are used. A high degree of crystalline faultlessness is also required, as faults in the crystal structure (such as stacking faults, dislocations, and twins) affect with the semiconducting characteristics of the material. Crystalline faults are a most important cause of defective semiconductor devices. The larger the crystal, the harder it is to achieve the necessary faultlessness. Current mass production processes use crystal ingots between 100 and 300 mm in diameter which is germinated as cylinders and sliced into wafers. There is a different process that is used for the preparation of semiconducting materials for integrated circuits. One process is termed as thermal oxidation, which arrangements silicon dioxide on the surface of the silicon. This is used as an access insulator and field oxide. Other processes are known as photomasks and photolithography. This process is what produces the modes on the circuitry in the integrated circuit. Ultraviolet light is used along with a photoresist layer formation a chemical change that procreates the modes for the circuit.

The next process that is required is the etching. From the previous step, the part of the silicon that was not covered by the photoresist layer can now be etched. Plasma etching is the main process that is typically used today. Plasma etching usually involves an etch gas pumped into a low-pressure chamber to produce plasma. A common etch gas is chlorofluorocarbon (Freon). A high radio-frequency voltage between the cathode and anode is what establishes the plasma in the chamber. The silicon wafer is placed on the cathode, which causes hitting it by the positively charged ions that are free from the plasma. The final result is silicon that is etched anisotropically. Diffusion is the last process. This is the process that gives the semiconducting material its desired semiconducting properties. It is known as doping also. The process presents an impure atom to the system, which generates the p-n junction. In order to get the impure atoms embedded in the silicon wafer, the wafer is first put in an 1100 degree °C chamber. The atoms are injected in and eventually diffuse with the silicon. After the process is completed and the silicon has reached room temperature, the doping process is done and the semiconducting material is ready to be used in an integrated circuit (Sze, Simon M. 1981).

A semiconductor photocatalytic efficiency of material has concerned considerable attention to both environment fields and energy application, it influenced by the photogenerated electron hole separation processes. Hence, developing metal/semiconductor heterostructures can reduce the rate of recombination electron-hole, in that way increasing the efficiency of photocatalytic the formation of heterostructures among the semiconductors with different majority carrier type is an alternative effort to increase the hole of electron lifetime, by making junction between n-type and p-type semiconductors a depletion layer at the region of p-n interfacial can be produced that induces an electric field. Some important major factors have been studied in controlling photocatalytic efficiencies and their optical properties, which highly depends on impurities, size, dopants, and morphology of the materials, instead of, the optoelectronic properties, and the performance catalytic of semiconductor materials also depend on the number of active sites present on the catalyst surface and also the surface area. So, morphology and size controlling of the photocatalyst require getting efficient, active sites and reproducible photocatalytic properties. The nanoparticles have been presented morphology and uniform size especially desirable in production of semiconductor material, as the synthesis of morphology, uniform surface area, and active sites photocatalytic properties (Kandjani et al. 2015).

Semiconductor materials are generally used in several fields including: transistor, diode, capacitor, thermistor, computer, rectifier hard disk, USB flash drive, graphics processors radar, solar panels, and satellite communications. Semiconducting nanotechnology with controlling size, structure, and orientation playing an important role in the fabrication and various applications such as photovoltaic cells, field-effect transistors, thermoelectric devices, memory elements, photodetectors, diodes, light emitting diodes, nanolasers, chemical and biological sensors (Reut et al. 2016). In addition, various techniques and methods have been used for preparation of semiconductor metals, such as deposition, using high-energy sources, deposition precipitation, and ultrahigh vacuum sputter coating, these techniques are used to produce nanoparticles with wide size distribution and non-uniform clusters. To overcome the difficulty of weak interactions between metal oxide and metal, various works have been made to modify and provide the better surface of metal oxide with an intermediate layer such as polymers, surfactants, or amorphous Si−OH polymers. These modifications provide new functional groups such as thiols,

amines and carboxylates, which introduce covalent linkages between metal oxide and metals (Pan et al. 2012).

Some generally used semiconductors and semiconducting materials and areas of use: copper (I) oxide (Cu_2O): diode in solar applications, copper (II) oxide (CuO): the sensor is in the solar battery, boron (B), indium (In), gallium (Ga): to form a p-type semiconductor, silicon (Si) and germanium (Ge): in making diode, transistor, integrate, antimon (Sb), phosphorus (P), arsenic (Ar): to make n-type semiconductor.

An important field of nanotechnology contains the manufacturing of nanostructure based gas sensors with high stability, selectivity, sensitivity, recovery time and improved response. These techniques are commonly used for producing nanomaterials, and also they were provided a great control for the physical properties of the products, such as size, shape, and composition. In best cases, metal oxides, which have a transducer role and receptor, are used as gas-sensing materials as their resistances of electrical will change correspondingly upon exposure to reducing gases or oxidizing gases. In the sensing process, specific interaction between target molecules and a metal oxide surface is required and also the materials should be in large ability to transfer the interaction induced alterations from the surfaces into a macroscopically accessible signal, typically, a change in the electrical resistance (Liu et al. 2012).

The most important problems that hamper the growth of society is the crisis of energy and environmental pollution, the researchers assumed that in order to solve these crisis of fossil fuel depletion, they used photocatalytic water decomposition, which uses solar energy to split water, producing clean hydrogen energy, while the photocatalytic degradation of toxic organic pollutants is thought to be an inexpensive and feasible way of addressing environmental issues (Zhu et al. 2010). On the other side, fossil fuels are the chief part of energy sources consumed on the world today. However, their burning products are causing the global problems, such as the ozone layer depletion, greenhouse effect, acid rains, and pollution, which are pretension a great danger for our environment and eventually for the life in our planet, therefore, the scientists and the researchers were tried to find an alternative energy sources to maintain the current life standards. Many scientists agree that replace to the hydrogen energy system. Hydrogen is a secondary

form of energy or an energy carrier. Although there are some production methods, hydrogen gas can be produced in large quantities by water electrolysis. The electricity needed for the electrolysis can be supplied by renewable energy sources such as solar cells (Solmaz et al. 2016).

Renewable energy sources have been a research field that has been researched frequently in order to meet the rising energy demand in our country and the world also has been carrying out serial production. When someone thinks of renewable energy, should be thinking of costs, clean, cheap and long lasting power unit. Such as life source water is an inexhaustible natural resource and hydrogen is a renewable, sustainable and clean energy source, the breakdown of hydrogen and oxygen water with minimal fuel consumption is one of the most important chemical processes related to energy. Solar energy is an important renewable energy source, considered as a major alternative to existing energy and environmental problems.

Solar cell power is also measured one of the cleanest of renewable energy resources, the public opinion, too, is particularly favorable to the use of solar energy, which seems to be without any environmental impact. A typical solar cell exists of n-type emitter, p-type emitter, front and back electrodes and an antireflective coating. The active n-type and p-type make up the p-n junction where generate electricity, to increase the total output. Solar cells strings are connected in series also to protect effective of the solar cells from stress of mechanical, weathering and humidity, by stringing the cell in a transparent bonding material that applied to a substrate; usually glass, but acrylic plastic, metal or plastic sheeting can also be used. It is common that excitons occurs in the active layer of organic solar cells, it has a distance of excitons migration are much small less than 20 nm, therefore, the distance for migration and diffusion to the interface of electron acceptors and electron donors in organic solar cells, it should be less than 20 nm to obtain best efficient of light conversion (Stoppato 2008).

Electrochemical techniques are multipurpose and powerful analytical tools, which are able to make available high sensitivity, low detection limits, accompanying to the use of low cost instrumentation which presents as an additional advantage relatively low operator training requirements. These properties make electrochemical techniques very

useful not only for routine analytical applications but also for fundamental physicochemical research such as interface processes, molecular interactions (Wang and Wiley 2001).

Electroanalytical methods involve the measurement of an electrical property such as potential, current, conductivity or electric charge which is directly related to the concentration of the analyte. Therefore, electroanalysis is based on the fundamental relationships obtainable between chemistry and electricity; it has been used in many areas such as industrial quality control, environmental monitoring, biomedical analysis, etc. The chief electroanalytical techniques are potentiometry, coulometry, voltammetry, and amperometry.

Potentiometry is based on thermodynamic relationships between the electrical potential measured at equilibrium conditions and the activity of some species in solution. In the electrochemical sense, equilibrium conditions (there is no current flowing across to the electrochemical cell). So, in potentiometry, information about the compounding of a sample is acquired by measuring electrical potential between two electrodes in absence of meritorious current. Analytical applications of potentiometry involve the detection of the endpoint in potentiometric titrations and direct potentiometry where the potential measured is used to make available the analyte concentration (P. R. Aranda et al.2009).

The main applications and advances in potentiometric methods involve direct potentiometry. Every electrochemical system required for potentiometric measurements includes a potentiometer which allows potential measurements and prevents the flowing of current between the electrodes; a reference electrode whose potential is constant and insensitive to the sample composition and an indicating electrode which potentiometrically responds to the analyte activity (Sawyer et al. 1995).

Electrodeposition is a technique low temperature process of energy used to make those materials which are used in computer chips and magnetic data storage systems with lower the cost and improve the performance of our information society. In addition, also used for producing those structures that used in a nanotechnology, nanobiotechnology based future (Bartlett et al. 2004).

Transparent conductive oxide film has high permeability in the visible region and is obtained from semiconductor materials with low electrical resistivity. Transparent conductive oxides such as ZnO, SnO_2, In_2O_3 and InSnO (ITO) as n-type materials are used in many optoelectronics systems have large applications. Cu_2O is material transparent conductive oxides with p-type conductivity, and by joining p-type and n-type, p-n obtain which very important materials for devices (Alkoy and Kelly 2005).

Copper has two stable oxides, cupric oxide (CuO) and cuprous oxide (Cu_2O). Both of them have main important, wide range of application and specific properties. The first oxide of copper is CuO it has p-type direct band gap (1.4 eV) semiconductor due to copper vacancies in the structure. With unique characterization, useful photocatalytic properties and photovoltaic properties, particularly, and special properties include low production cost, non-toxic, electrochemical activity, abundance constituents in nature and chemical stability, in addition, possess significant role in the studies of metal semiconductor, metal interlayer semiconductor, in the last decades Schottky diodes. Thus, by inserting an interlayer between the semiconductor and metal, the interfacial layer can be modified electrical parameters of metal semiconductor structures (Erdoğan et al. 2010). The numerous development technique and methods including catalysis electrodeposition, spin-coating, sol–gel, solvothermal, hydrothermal and thermal oxidation been used to synthesize CuO nanoparticles used in large various applications such as gas sensors, catalysis, bio sensing, high temperature superconductors, magnetic storage media, solar cells, batteries, electronics, electrode materials, field of emissions and lithium-ion electrode materials. It has been reported the important publications on the photocatalytic and as an antimicrobial activity of CuO nanostructures (Sathyamoorthy and Mageshwari 2013).

The second oxide of copper is cuprous oxide which is an important p-type semiconductor material, it has the major applications of Cu_2O are use as transparent active p-type layers performance in conversion light to electrical energy in solar cells, field effect touch screens, transistors, and gas sensors. In addition, other applications in photo catalysis, photo electrochemical water splitting, solar energy conversion, biosensors, and coherent propagation of excitons. Especially, the resulting of high electrocatalytic activity from multi electron oxidation mediated in enzyme-free glucose sensors by surface metal oxide

layers. They play an important role in the selective surface modification for example passivation, hardening, coloration in the form of coatings of various substrates. Although, studied numerous nanostructure of Cu_2O materials with difference morphologies, such as nanowires, nanoparticles, nanocubes, nanosheets, hollow nanostructures and nanospheres, moreover, the high crystalline Cu_2O nanofilms have been prepared by spin coating and annealing combined with a simple chemical method (Feng et al. 2014).

Cuprous oxide is one of the well-known p-type narrow direct band gap 2.1 eV semiconductors. It has many advantages of non-toxicity, low cost and abundance of its starting material. It has large application include of solar cells, photo catalysis, and photo electrochemical water splitting, due to its favorable absorption in the visible range (Li et al. 2014).

Cu_2O semiconductor, with special magnetic and optical properties, has attracted increasing attention in different application include potential photovoltaic material, photocatalysis reactions, solar energy conversion, photocurrent generation, a stable catalyst for photo activated splitting of water or other liquids under visible light irradiation. Cu_2O nanostructures with different structures, size and surface morphologies such as nanorods, nanocubes, nanooctahedron, and nanospheres, have been synthesized by various methods such as vacuum evaporation, wet chemical, thermal relaxation, electrodeposition, solvothermal method, complex precursor surfactant assisted route, and their surface-dependent catalytic, electrical and other properties have been studied (Kandjani et al. 2015).

Cu_2O can be prepared by non-vacuum techniques, such as thermal oxidation of Cu sheets and electrochemical deposition. It is a native p-type semiconductor, due to a high concentration of negatively-charged copper vacancies; this is combined with a high absorption coefficient for energies, high majority carrier mobility and also large minority carrier diffusion length up to several micrometers (Malerba et al. 2011). Several techniques and methods have been used for synthesizing cuprous oxide films with both high and low temperature contain thermal oxidation, hydrothermal, reactive magnetron sputtering, and electrodeposition (Abdellah et al. 2016).

In vitamin supplements and over-the-counter medicines, copper oxide is used as a safe copper source. Furthermore, because of its cosmetic and microbial properties, the cupric oxide is also found in consumer products such as socks and pillow cases. Depending on the skin, the risk of skin sensitivity is considered extremely low. The cupric oxide is used as a pigment in the production of red, blue and green (sometimes gray, embossed or black) glazes in the ceramic field. Copper oxide is also used to make the ammonium hydroxide solution used to make the rayon, and sometimes as a biomass reinforcing against the lack of copper in the animals.

In addition, the cupric oxide is used as a cathode in wet cell batteries using lithium peroxide as an anode and lithium perchlorate mixed with dioxane as an electrolyte. Copper oxide can be used for the production of other copper salts. It is also used when welding with copper alloys. Another use is to replace iron oxide in the termite. Termite reaction is used in various fields from fire to low explosive use. Another area of use is the disposal of waste materials. Copper oxide can be used to oxidize and safely destroy dangerous substances such as halogenated hydrocarbons, cyanide, dioxins and hydrocarbons (URL-7 2016).

P-type conduction property of Cu_2O is due to the formation of Cu vacancies and delocalized holes after the removal of copper atoms from the lattice through oxidation reaction as shown these two reactions (Nolan et al. 2006):

$$Cu^{+2} + e^{-} \rightarrow Cu^{+} \quad (1.1)$$

$$2Cu^{+} + OH^{-} \rightarrow Cu_2O + H^{+} \quad (1.2)$$

It is clearly seen that reaction (1.2) depends on the OH^{-} concentration (i.e. pH) of the bath. At low pH values presence of excess Cu^{+} ions may favor the formation of Cu rich or O deficient (i.e. having O vacancies) Cu_2O films. Thus high density of donors can be expected and therefore the film may become n-type (Siripala 2008). When the pH of the electrolyte is higher and lower concentrations of Cu ions, there will be a tendency to produce Cu_2O films with Cu vacancies. In other words, acceptor density will become significant and then the films become p-type. It is clear that the OH^{-} concentration value

does not independently determine the conduction type but according to equation (1.2) it should depend on the concentration of the Cu^{+}. On the other hand, it is important if there is a possibility of controlling the defect concentration of the Cu_2O film by the pH of the depositing bath and the Cu^{+} concentration, This is important because Cu^{+} vacancies produce p-type conductivity while oxygen vacancies could produce n-type conductivity in Cu_2O films (Jayathileke et al. 2008).

In this thesis, photoactive materials containing Cu_2O with high quality and stability were prepared by using economical, simple and reliable electrodeposition method based on underpotential deposition (UPD). Prepared materials were characterized using XRD, SEM, EDX, UV-Vis spectroscopy and electrochemical techniques. The photoelectrocatalytic performances of Cu_2O semiconductor electrodes depending on electrodeposition time were determined and the change in photoelectrocatalytic activities was studied comparatively.

2. LITERATURE REVIEW

A study was conducted to quantitatively investigate the effect of the electrode temperature on the optical and photoelectrochemical properties of Cu_2O film (Lin et al. 2014). Three different temperatures (35, 50 and 65 °C) were taken into account. P-type Cu_2O thin films have been successfully prepared on copper foil substrates by electrochemical deposition at -0.30 V in an alkali bath containing copper sulfate and lactic acid at temperatures ranging from 35 to 65 °C. These films have distinct morphology and crystal structure. They exhibit different optical and electrical properties. The film deposited at 50 °C and at 65 °C sprang up from microparticles, while the Cu_2O film deposited at 35 ° C was formed from nanoparticles. This low temperature coated Cu2O films have a smaller pyramid-like crystal size and higher photoluminescence properties. These properties make it possible to prepare Cu_2O film with better electrochemical performance at -35 °C with -0.4 V photoacid densities. All films have identical band gap energies and are 2.17 eV, but have different fouling and defects at different concentrations. The energy level diagrams of the films have been examined. The film at 35 °C gave a much denser PL signal than the films prepared at 50 and 65 °C. In addition, Raman spectroscopy was used to confirm Cu_2O film compositions. The properties of Cu_2O films are closely related to the structures of the film compositions.

CuO nanoparticles were prepared by thermal decomposition method and characterized by XRD, TEM and UV-Vis spectroscopy (Dolui et al. 2013). The particles obtained are spherical and have an approximate particle size ranging from 15-30 nm. The antioxidant behavior of the synthesized CuO nanoparticles was assessed by free radicals of 2,2-diphenyl-1-phenylhydrazine hydrate (DPPH). Free radical scavenging activity of CuO nanoparticles was monitored by UV-Vis spectrophotometry. CuO nanoparticles are relatively higher than other metal oxide nanoparticles. It showed up to 85% free radical scavenging activity within 1 hour. CuO nanoparticles are promising antioxidants in polymer processing and non-biological systems. The antibacterial activity of CuO

nanoparticles has been tested against several bacterial groups with genetic differences between them. With a concentration increase of CuO nanoparticles, there is a significant reduction in bacterial growth. CuO nanoparticles showed bactericidal activity against Escherichia coli (bacterial causing bacteria in the large intestine) and Pseudomonas aeruginosa with effective antioxidant activity.

A very high level of formaldehyde-sensitive gas sensors composed of CuO nanocouples were produced and characterized using various methods (Lee et al. 2014). The Cu_2O nanocouples are prepared by wet, easy and mass-producible polyol processing. CuO nanocubes are prepared by oxidation using heat oxidation in air. CuO nanocube gas sensors are then successfully produced on the silicon surface. HCHO gas response properties such as sensitivity, reproducibility, linearity and recovery have been discovered at different operating temperatures (250-350 °C). The synthesized nanocapsules were monodispersed and the average edge size was about 90 nm and the average pore size was about 52 nm. Given this appropriate sensitivity and rapid response, it has been determined that the gas sensors have an operating temperature of 300 °C. At the working temperature, CuO nanocube gas sensors reacted to high HCHO gas. That is, in the range of HCHO gas concentration between 0.05-3 ppm, the logarithmic characteristic is outstanding. The gas sensors showed excellent reproducibility and a very low limit at 250 °C 6 ppb (coefficient of variation between 800 ppb and 1.17% at 300 °C). In addition, among the available test gases such as C_6H_6, NO_2, CO, CO_2, NH_3 and HCHO in the ambient atmosphere, CuO nanocube gas sensors showed the most severe reaction to HCHO gas at 300 °C. This research has shown that using oxides of CuO nanocubes may be an alternative platform for HCHO gas detection and has opened a new path for the development of improved formaldehyde sensing materials using mass-producible polyol processing.

CuO nanocrystals were prepared by sequential ionic layer adsorption and reaction method, which is a simple and low cost technique and the effect of deposition cycles on the physical properties of materials was investigated (Sathyamoorthy and Mageshwari 2013). Preparation conditions such as concentration, pH, adsorption, reaction and rinse duration are optimized to obtain homogeneous and high quality CuO thin films on glass surfaces. XRD studies have shown that all films exhibit multicrystalline properties with a

monoclinic crystal structure. FTIR and Raman studies confirm the formation of single-phase CuO. Here the characteristic vibrational mode of Cu-O is defined. Scanning electron microscopy studies have shown that elongated particles of bar-shaped particles are formed by scattered growth. XRD, FTIR and Raman studies confirm the nanocrystalline and single phase formation of CuO thin films. Optical absorption studies showed the presence of direct band pass in CuO thin films and the increase in the thickness of the thin films revealed that the band gap energy decreased from 2.48 eV to 2.31 eV. The PL spectrum exhibited emission peak points between 397 nm and 532 nm with an average band edge emission of around 468 nm.

CuO nanostructures with different shapes were prepared at low temperatures using a hydrothermal technique without the use of templates and surfactants (Wang et al. 2014). The effects of temperature, time and temperature on the nanostructure growth have been investigated. The feather-like, rod-like morphology dimension of the CuO nanoparticles, such as flower, can be adjusted by adjusting the reaction parameters including the concentration of the reagent, the precipitant, the reaction temperature and the reaction time. The samples are characterized by FE-SEM and XRD. At the same time photo dissociation test and UV-Vis spectroscopy were performed. Photo degradation rate for methylene blue can reach 92.1%. The calculated optical band gap of the nanotubes is about 5.89 eV. The results show that CuO nanostructures have a monoclinic structure with a single crystal phase. However, the structure and morphology of CuO nanocrystals can be controlled by changing the remote concentration. In addition, Ostwald's maturation mechanism has been proposed to explain the formation of CuO nanostructures in this work.

The non-enzymatic glucose sensor coupled with CuO nanoparticles was prepared using a multi-wall carbon nanotube array (MWCNTs) vertically aligned with highly stable and sensitive properties (Gunasekaran et al. 2010). A simple and rapid two-step electrodeposition technique was used to prepare CuO-MWCNTs nanocomposites. The MWCNTs cluster was prepared by catalytic chemical vapor deposition on the Ta substrate. First, Cu nanoparticles were deposited on MWCNTs at constant potential and then oxidized into CuO. The electrocatalytic activity of the CuO-MWCNTs sequence was investigated under alkaline conditions using voltammetry and chronoamperometry. The

sensor response time is 2 s and the detection limit is less than 800 nM. CuO modified MWCNTs showed significantly higher electrocatalytic activity against GIc oxidation with higher current response and lower oxidation potential than MWCNTs that were not modified. These performance characteristics are thought to be a potential candidate for routine Glc analysis of the CuO-MWCNTs electrode when combined with production for Glc in the presence of common parasite, long-term stability, good reproducibility, rapid response and excellent specificity.

The CuO particles were prepared using a simple and rapid hydrothermal method without using organic template as ball-shaped crystals (Naskar et al. 2014). XRD showed the crystallization of $Cu_2(OH)_2CO_3$ and the monoclinic CuO phase for the specimens prepared at 300 °C. The BET surface area, the total pore volume, and the average pore diameter of the samples were found to be 67.4 m^2g^{-1}, 0.39 cm^3g^{-1} and 23 nm, respectively. Microstructural analysis indicates a hood-like structure consisting of self-assembled particles (length 210 μm, diameter 200-300 nm). The single crystal structure of the particles was confirmed by SAED and HRTEM images. A temporary formation mechanism has been explained. Catalysis, magnetic storage, field emission emitter, solar cell etc. are likely to find potential applications in their areas.

CuO microspheres have been successfully prepared by the hydrothermal process using large quantities of copper acetate as a reagent in the presence of polyvinyl pyrrolidone (Qiao et al. 2014). The hollow CuO cage is formed by many nanobots at 400 nm wall thickness. The surface area of hollow CuO microspheres was measured as 25.7 m^2/g by BET nitrogen adsorption method. It is thought that hollow microspheres may be an advanced material for potential applications in the field, such as short time gas sensing optical materials. At the same time, it has been found that the unique regular performance shows excellent electrochemical performance for lithium ion batteries.

Cu_2O/CuO nanostructures were prepared by direct crystallization in the presence of sodium borohydride without using any oxidant or surfactant (Li and Fan 2011). Microstructures and shapes of Cu_2O/CuO nanowires were investigated by electron microscopy field emission, XRD and TEM. The CuO microstructures from the nanoclusters or dense structures of the nanostructures were achieved using $NaBH_4$

concentration. According to the results, $NaBH_4$ has acted both as an alkaline factor and as a reductant for the unusual development of CuO nanostructures. A possible growth method in which the first building units were controlled within three-dimensional flower-like structures was proposed. After simple surface modification with the sodium borate salt, the resulting membrane exhibited hydrophobic or even super hydrophobic properties due to their specific surface nano/microstructures. According to the results, advantages such as fabrication and manufacturability of stepped CuO structures are evident. For potential applications such as advanced catalysts, clean surfaces and sensors, this promising approach is expected to be applicable to the composition of functional CuO-based materials.

CuO nanocrystals with photocatalytic properties were prepared using an electrochemical method (Mukherjee et al. 2011). Structural characterization showed the formation of a cubic phase for both Cu and CuO films. However, as an effect of the annealing of the crystals it was found that the shapes can be changed to cubic nanocrystalline. XRD, SEM, UV-Vis, PL and Raman analyzes were performed. The photocatalytic effect of the prepared CuO films was determined by measuring the discoloration of Rose Bengal dye to find a potential application in waste water treatment. The photo degradation kinetics was obtained by subjecting to about 84% degradation after 260 minutes.

Using direct current magnetron sputtering technique, Cu_2O thin films were prepared by precipitation of copper target on quartz substrates in a mixture of oxygen and argon gas (Zhang et al. 2009). The effects of partial pressures of oxygen and gas flow rate on the properties of the films were investigated. The changing oxygen partial pressure leads to the synthesis of Cu_2O, Cu_4O_3 and CuO with different microstructures. When the gas flow rate is below 80 sccm and a constant oxygen partial pressure of 6.6×10^{-2} Pa, a single-phase Cu_2O films can be obtained. The deposited Cu_2O films were found to have a very high optical absorption in the visible spectrum below 600 nm and exhibited photocatalytic reactivity under visible light.

As a new anode material for lithium ion batteries, Cu_2O thin films were prepared by electrodeposition technique (Fung et al. 2004). Copper oxide was successfully electrochemically deposited with the pure cubic phase. The results of the combined

electrochemical cell tests indicated that the electrodeposited copper oxide film had high electrochemical capacity and allowed excellent cycle retention. After 50 cycles, it was observed that the capacities were still sustainable at about 220 mAh/g and that the decay was not significant outside the first cycle. The Cu_2O film, which is dense and homogeneous by the electrochemical deposition, has been successfully deposited on the $Pt/Ti/SiO_2/Si$ layer without any subsequent heat treatment. SEM and TEM observation showed good adhesion properties between the film and substrate.

The transparent p-type Cu_2O thin film was manufactured by a process comprising a thermal reaction, deposited on the glass substrate, with a thickness of 50 nm, successfully (Sato et al. 2012). The precursor solution was prepared by the reaction of an isolated Cu^{2+} complex of dibutylamine with ethylenediamine N, N, N′, N′-tetraacetic acid in ethanol. At a flow rate of 1.0 L min^{-1}, precursor film heat treatment at 450 ° C for 10 minutes in Ar gas resulted in a precise cubic lattice cell parameter with a crystallite size of 8(2) nm of Cu_2O thin films. The specified a=0.4265 nm is characterized by XRD. In the case of Cu_2O film, O 1s and Cu can be bound to $2p_{3/2}$ level. X-ray photoelectron spectroscopy peak points were found to be 532.6 eV and 932.4 eV, respectively. The average grain size of the deposited Cu_2O particles was observed with a 200 nm field emission scanning electron microscope. When the Cu_2O transparent thin film absorption spectrum was evaluated, it was 2.3 eV when the optical band edge was assumed to be directed semiconducting. Thin film Hall Effect measurements have shown that Cu_2O thin film is a typical single-phase p-type semiconductor with a cell concentration of $1.7x10^{16}$ cells at ambient temperature and a cell activity of 4.8 $cm^2V^{-1}s^{-1}$. Activation energy from the valence band at the receiver level determined from the Arrhenius graph has been 0.34 eV. FTIR, TG-DTA, XRD, XPS, FE-SEM, UV-Vis spectroscopy and Hall Effect measurements were used to provide detailed characterization of the composition of Cu_2O thin films adhered to a glass bottom plate without Na.

Cu_2O films were prepared on flexible copper and Mo substrates in a basic environment by the electrochemical deposition method (Mathew et al. 2011). Such deposited films revealed that the films contained only the Cu_2O phase by p-type and XRD analysis. The thicknesses of the films are calculated from the interference fringes of the reflection spectra. Au/Cu_2O Schottky diodes were prepared by spraying Cu_2O films on Mo

substrate as a layer of very pure gold with a thickness of 15 nm. Possible optical transitions near the tape edge were calculated from the spectral response of the device. It showed that there is a linear dependence of temperature on the calculated tape gap at different temperatures. The direct transition temperature dependence of 2.493 eV observed at room temperature is shown. Electrode position is a suitable method for preparing Cu_2O films on wide area substrates.

Copper oxide thin films were obtained by electrodeposition method on Cu and tin oxide coated glass surfaces with cubic morphology and polycrystalline structure (Mahalingam et al. 2005). The optimum range of the accumulation parameters has been experimentally investigated. XRD studies revealed the formation of single-phase cubic Cu_2O films at a potential range of -0.355 to -0.555 V vs. SCE. Studies have shown that films with a single-phase cubic crystallinity improved at an optimum pH of 9.0. The preferred orientation of the (200) cubic Cu_2O peak region was found to increase with bath temperature between 30-70 degrees C. The resistance, band gap and activation energy of a typical Cu_2O film region are estimated to be $5x10^6$ Ωcm, 1.99 and 0.85 eV, respectively. During the annealing it was observed that there was no change in the band gap below 350 °C. Annealing, however, increases the crystallite size and reduces the film in electrical resistance to 10^7 to 10^3 Ωcm. The band spacing from 1.97 to 2.25 eV and the black color change from the red brick color of the color showed the conversion of Cu_2O to CuO during annealing at 450 °C. The preferred orientation, grain size and annealing effects on optical band gap have been studied. The energy conversion efficiencies of p-Cu_2O films deposited and annealed as photocathodes in photo electrochemical solar cells were investigated and the results are discussed. Auto electrochemical solar cell work using p-Cu_2O as photocathode exhibited a higher conversion efficiency for annealed films.

Copper and copper oxide thin films were prepared using an electrodeposition method in an acetate bath (Wijesundera et al. 2006). Voltammetric curves were used to explore growth parameters such as potential for deposition, pH and canyon temperature. Structural, morphological, optical and electronic properties of potentially dependent films were investigated by XRD measurements, scanning electron micrographs, absorption measurements dark and open-voltage typologies. Single-phase Cu thin films with greater

deposition potential than -700 mV Vs SCE have been produced. The photo reaction developed in a photoelectrochemical cell was produced by a thin film of Cu_2O prepared at -400 mV Vs SCE. This study demonstrates that a single deposition chamber can be used to deposit both Cu and Cu_2O separately and a mixture of Cu-Cu_2O with control of the deposition parameters. Studies have shown that single-phase Cu_2O and Cu thin films can potentiometrically electroplating sodium acetate and copper acetate containing an aqueous solution in the range of 0 to -300 mV Vs SCE and -700 to -900 mV Vs SCE potentials, respectively. It is possible to coat Cu and Cu_2O at the same potential in the SCE potential range of 400 to -600 mV Vs. For Cu_2O thin films of cubic shape at about 1-2 μm, -200 mV Vs potential for deposition around the SCE may be possible. Light and dark current-voltage measurements in a photoelectrochemical cell revealed that the photoactivity of Cu_2O thin films in photoelectrochemical can be improved by microscopically scaled random Cu deposition on Cu_2O thin films.

Cu_2O thin films were prepared using a reactive magnetron sputtering system (Zhang et al. 2013). Band spacing, refractive index, mobility, hole density and electrical conductivity in films are also investigated. Cu_2O thin films are manufactured in rich N and rich O conditions. Films deposited under oxygen-rich conditions have narrow bandwidth and high electrical conductivity, while films produced under nitrogen-rich conditions exhibit broadband spacing and low electrical conductivity. The results of the density functional theory are presented to explain the gas dependence of the band gap. A theoretical model based on the Fermi-Dirac statistics shows that high electrical conductivities in the film are due to receiver levels below the Fermi level. The thin films were produced under rich N and O conditions. The optical and electrical properties of these films have been investigated with permeability measurements, band-interval simulations and refractive index calculations. Hall measurements have shown us that films made in rich N conditions have a wider band gap and lower conductance than films deposited under rich O conditions. These findings are thought to be useful for optimizing the performance of Cu_2O thin films.

Growth of Cu_2O thin films was investigated on the FTO surface by electrochemical deposition (Ryu et al. 2014). The effect of annealing temperatures and annealing times on the morphological, structural, photoelectrochemical and optical properties of Cu_2O thin

films formed with pH value 11 was investigated. Cu_2O thin films at pH 11 show higher photoconductivity. It has been found that the properties of these Cu_2O thin films depend on the degree of crystallization and morphology. Cu_2O thin film with the best structural and photoelectrochemical properties was obtained at 200 °C annealing time in vacuum for 30 minutes. In this case, the highest (111)/(200) XRD peak intensity ratio of annealed Cu_2O thin films is 52.5 and the highest photoacid density is 2.90 mA/cm^2.

Cu_2O thin films with adjustable growth orientations on glass and silicon surfaces were prepared using reactive sputtering and crystal growth was investigated (Pierson et al. 2014). The effect of certain orientations on subsequent crystal growth during the growth phase of crystal growth, which was initially observed, has been studied in detail. Among various coating conditions, it has been found that the total pressure has a strong influence on the preferential orientation of Cu_2O films. Accordingly, the (100) orientation is at low pressure and the (111) orientation is at high pressure. Cu_2O films grow at a low pressure (0.5 Pa) with a (100) texture orientation, while a (111) texture orientation at high pressure (1 Pa) is determined. Furthermore, the texture of the deposited films is influenced by the first Cu_2O layer acting as a continuous core layer. Effectively, a Cu_2O thin film with many textures with controlled orientation can be formed independently of deposition conditions, using a two-stage deposition procedure. Provided that it has a sufficient thickness, this layer functions as a core layer which determines the crystal orientation of a second layer after it has been exposed to air or before it has been deposited and without accumulating on the surface thereof a certain cleaning. High-resolution transmission electron microscopy analyzes demonstrate that a homoepitaxial growth occurs with the core layer, which has a microstructure consisting of single crystal groups.

Cu_2O thin films were prepared on fluorine doped SnO_2 glass, Cu foil and Ti foil with the help of cetyltrimethyl ammonium bromide using chemical bath deposition technique (Yu et al. 2011). This surfactant, cetyltrimethyl ammonium bromide, has been found to play an important role in the formation of nanosphere morphology. The specimens were characterized by XRD, SEM and UV diffuse reflectance spectroscopy. The results show that Cu_2O films prepared in the presence of cetyltrimethyl ammonium bromide in the chemical bath precipitation system are composed of nanobubble arrays. In the absence of cetyltrimethyl ammonium bromide, nanosphere-shaped Cu_2O films were observed. The

concentration of cetyltrimethyl ammonium bromide is important for the morphology controlled synthesis of nanobubble Cu_2O films. Diameter ratios in different lengths and nanobubble row density are both due to substrate and cetyltrimethyl ammonium bromide concentration. A possible mechanism for Cu_2O nanobubble film formation is proposed. In addition, UV-Vis absorption is much better for Cu_2O nanobots. The photovoltage produced under visible light for Cu_2O nanobubble films is higher than that produced for Cu_2O nanoclay films. Although Cu_2O nanobots can absorb visible light on Ti foil, copper oxide exhibits better and more stable photoelectrochemical properties on Cu foil than other surfaces. This work has been shown to be extremely useful for a device to be fabricated with Cu_2O nanostructure base.

CuO nanoparticles were prepared by thermal decomposition and characterized by XRD, TEM and UV-Vis spectroscopy (Dolui et al.2013). And also nanoparticles are promising antioxidants in polymer processing and non-biological systems. The antibacterial activity of CuO nanoparticles has been tested against several bacterial groups with genetic differences. With increasing concentration of CuO nanoparticles, there is a significant reduction in bacterial growth. CuO nanoparticles exhibited bactericidal activity against Escherichia coli (bacterial infection in large intestine) and Pseudomonas aeruginosa with effective antioxidant activity. A very high level of formaldehyde-sensitive gas sensors consisting of CuO nanocouples were produced and characterized using various methods (Lee et al. 2011).

Electrodeposition is a process as a low cost, low temperature, and thin film synthesis method. Those compounds that related to the formation of photovoltaics have been successfully grown using electrodeposition since the 70’s. Kroger et al. (1978) reported that co-electrodeposition as a classic methodology used for CdTe deposition in his work. The co-electrodeposition technique is simple, low-cost and given the right solution chemistry. This method has been formed many binary compounds at a controlled potential or current in a single solution containing precursors for both elements. The transition metal oxides such as (Fe, Co, Ni, and Cu) had been used, on the other hand, the innovation of thin film lithium batteries with high storage capacity and cost-effective anode materials, because these materials have the ability to reverse store high Li through a heterogeneous conversion reaction.

The key challenge for CuO and Cu_2O practical use in thin film lithium batteries is the improvement of their high rate capacity and cycling performances (Barreca et al. 2012). In studying the preparation and application of CuO nanowires (NWs), the mean length of CuO NWs was found to increase from 0.4 μm to 2.8 μm and 6 μm, respectively (Chang et al. 2011). After oxidation, the initial copper film thickness increased from 0.5 μm to 1 and 2 μm. At the same time, CuO is p-type, so CuO NWs resistance is increased with increasing relative humidity. Furthermore, it can be seen that with a larger copper film thickness at the beginning and thus an average longer CuO NW length, the samples could provide a larger sensor response.

3. MATERIALS AND METHODS

3.1. Materials Used in Laboratory Studies

3.1.1. The Used Chemicals

Copper sulphate pentahydrate ($CuSO_4.5H_2O$), sodium sulphate (Na_2SO_4), lactic acid ($C_3H_6O_3$), sodium hydroxide (NaOH), sulfuric acid (H_2SO_4), ethanol (C_2H_6O), acetone (C_3H_6O).

3.1.2. Instruments and Devices Used in Works

Precision balance: Denver Instrument SI-234
PH meter: Orian 3 Star
Ultrasonic mixer: Apple S 60 H
Deionized water device: Human Power 1
Electrochemical analyzer: CHI 6096 E
X-ray diffractometer (XRD): Rigaku Ultima IV
Scanning electron microscope (SEM): JEOL JSM-6510
Energy dispersive dpectrometer (EDX): JEOL JSM-6510
UV-VIS-NIR spectrophotometer: Shimadzu UV-3600
Solar simulator: Solar Light 16S-002

3.1.3. Materials Used in Electrochemical Studies

Electrochemical processes that make up a significant part of the work; analyzed substance, solvent, electrolyte and an electrode from an electrochemical cell and an electrochemical device known as potentiostat/galvanostat. We need to pay attention to the

selection of materials to be used for electrochemical studies. The particulars are mentioned below.

3.1.3.a. Properties of Solvent and Electrolyte

Starting with electrochemical studies, first it is necessary to investigate the chemical and physical properties of the solvent in detail. The solvents are used at a high degree of solubility, high electrical conductivity and very high purity. It should have dielectric constant, and should not enter into reaction. Furthermore, if pure water is used as the solvent, must be distilled water or higher purity production ultrapure water systems use. We used GFL 2008 brand deionization system in our studies.

3.1.3.b. The solutions

In our studies, we found that aqueous basic solutions containing 0.02 M $CuSO_4$, 0.2 M Na_2SO_4 and 0.3 M lactic acid solution, such as an environment that prepared by semiconducting materials were used by electrochemical method. The pH of the solutions is 9 that prepared by adjusting with pH meter using NaOH and H_2SO_4.

3.1.3.c. Electrochemical Cell

Electrochemical reactions can be performed in cells with two or three electrodes. Both of the cathode electrodes and anode electrodes are immersed in an electrolyte solution. Thus, the oxidation/reduction (redox) reactions take place, it’s clear that the reduction reactions take place in the cathode electrode, and also the oxidation reactions take place in the anode electrode. In addition, usually the electroactive in cells consisting of three electrodes dissolving the compound and the electrolyte dissolved in the solution, the counter and reference electrode (Goodridge and King 1974). Another important factor is the use of unfractionated cells where the three electrodes are placed in separate compartments in electrochemical processes and the opposite, the study, in which the reference electrode is placed in one compartment as shown in (Figure 3.1).

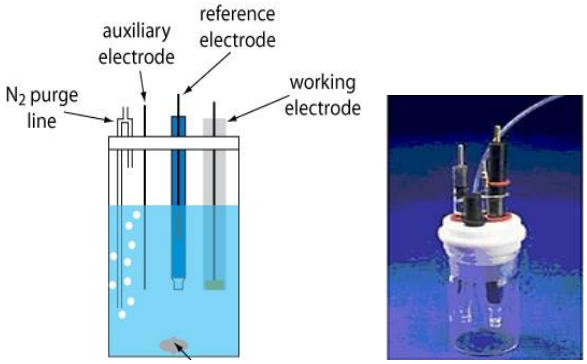

Figure 3.1. Electrochemical cell

3.1.3.d. The Electrodes

In our studies, we used three kinds of electrodes: reference, counter and working electrodes reference electrode, is one of the electrodes that have a half-cell knowing and fixed potential, with properties that is independent of its composition of electrolyte desired. These electrodes are used for potentially controlled electrolysis and voltammetry techniques; therefore, the reference electrode should be used so as to determine the potentials (Skoog et al. 1998). As well the reference electrode must be easily prepared, stable, with a specified current range. It must be having reversely and should not change over time. Generally, reference electrodes are silver silver chloride (Ag/AgCl) and saturated calomel reference electrode (SCE) used (Erdoğan 2009).

In our studies, Ag/AgCl and SCE reference electrodes used in the electrochemical preparation of Cu_2O photoelectrodes and photoelectrochemical studies, respectively. Some good properties of Calomel electrode: it's very easy prepared because of the ease of preparation of analytical chemists an electrolyte mercury-mercury chloride reference electrode; mercury and calomel in (Hg_2Cl_2), potassium chloride (KCl) solution formed into a platinum wire for external connection. An immersed half-cell is used as shown in (Figure 3.2). The potential of this half-cell depends on temperature and potassium chloride concentration of the reference electrode.

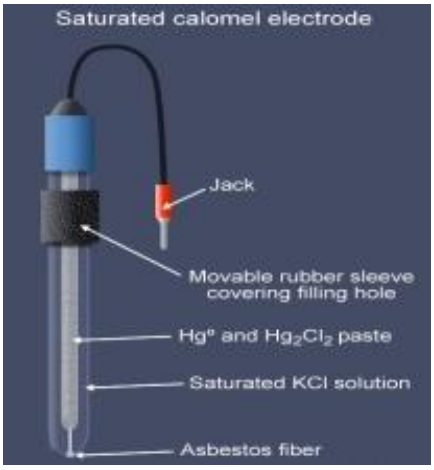

Figure 3.2. Saturated calomel electrode

The potential of saturated calomel electrode is 0.224 V due to faulty potential connection in case of potential connection to standard hydrogen electrode, liquid connection. However, when there is no fluid connection, this value is around 0.241 V (URL-1 2015). Figure 3.3 shows the potential change as a function of temperature. The potential values of the calomel electrode versus the standard hydrogen electrode (SHE) at 0-100 °C,

$$E_T = 0{,}244 - 0.00072\ (T - 25) \tag{3.1}$$

According this Equation (3.1) the potential change as a function of temperature as shown in Figure 3.3 at (12-50 K), on the other hand, the potential of the reference electrodes can change over the time, it should be preserved in a solution.

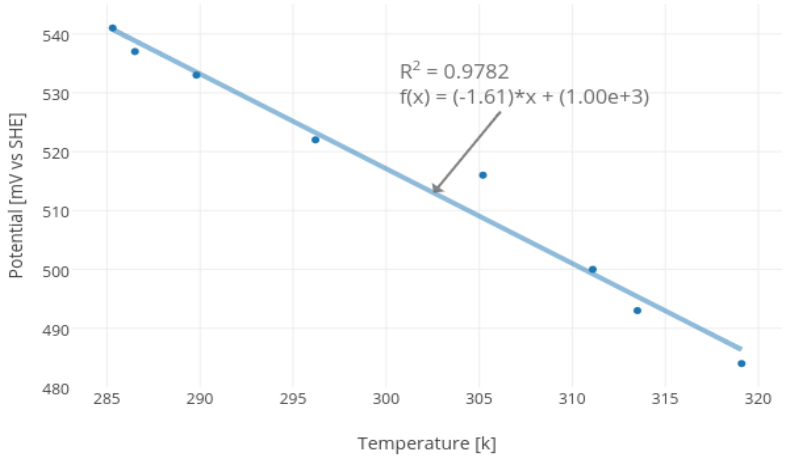

Figure 3.3. Change of electrode potential with temperature

The Ag/AgCl reference electrode was obtained by immersing Ag in an agitated solution after agglomeration with AgCl in the electrolytic solution (Figure 3.4).

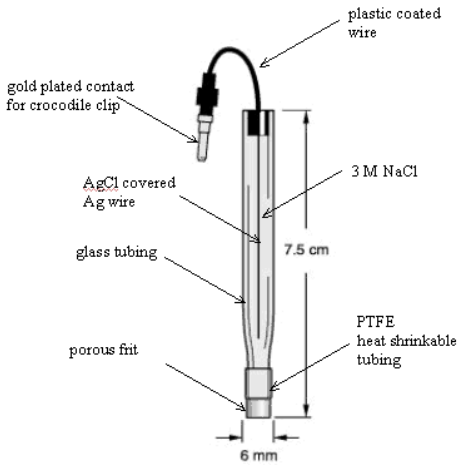

Figure 3.4. Ag/AgCl reference electrode

The potential of Ag/AgCl electrode is 0,222 V against standard electrode potential SHE. This value for SCE is 0.268 V. On the other hand, the concentration of KCl affects the electrode potential for both Ag/AgCl and SCE. For example, when the molar concentration of KCl for the calomel electrode is taken as 1.0 and 0.1 M, the voltages at 25 ° C are 0.282 and 0.334 V, respectively. Generally, Ag/AgCl electrodes can be used when working above 60 °C with calomel electrodes.

The working electrode is the most important part of the electrolysis system. By the way, the counter electrode has no effect on the reaction occurring in the working electrode. And also the counter electrode is used to complement the circuit and feeds the working electrode with electrons. For the more, a small current is observed in the counter electrode due to the non-process electrolyte types in the working electrode. Therefore, the counter electrode process is not interested. Several uses of platinum wire as counter electrode are because of its nature inert in electrochemical studies as shown in (Figure 3.5).

The working electrode is the electrode at which the analyte is oxidized or reduced. The potential between the working electrode and the reference electrode is controlled.

Electrolysis current passes between the working electrode and a counter electrode. The working electrode acts as an anode material in which an oxidation reaction takes place during oxidation in an electrochemical cell, and also cathode material during which the reduction reaction takes place during reduction. Moreover, the preference of the cathodic and anodic working electrode is important (Weinberg 1972). For this reason, surface morphology and activity must be taken into account in the preference of the electrode material. In our studies, ITO (indium tin oxide) coated glass was used as the working electrode, platinum wire was used as the counter electrode, and Ag/AgCI and SCE were used as the reference electrode.

Figure 3.5. Platinum counter electrodes

3.1.3.e. Potentiostat

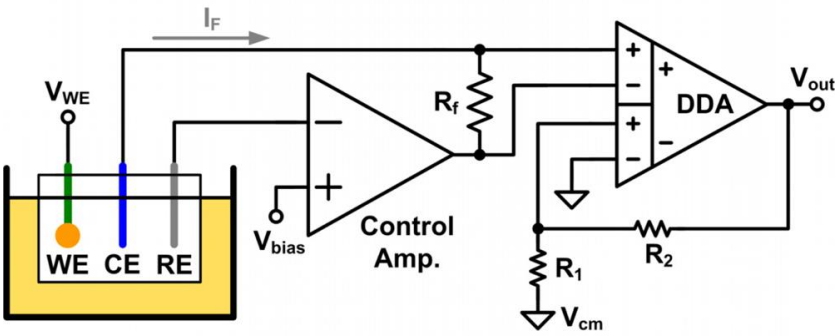

Figure 3.6. Schematic representation of potentiostatic components used in electrochemical studies

Potentiostat is an electronic device that regulates the potential of the working electrode versus the reference electrode. This is used in potentially controlled electrolysis. The

linearly scanned potential generator, similar to the integration circuits, is the signal source as shown in Figure 3.6.

The output signal from the source first comes to the potential control circuit. And also the electrical resistance is very large (> 10^{11} Ω) for a small amount of current flow in the control circuit containing the reference electrode, this ensures that all of the current from the source is transferred from the opposing electrode to the working electrode. In addition, in the potentiostat process, the current measuring circuit is connected to the working electrode. Moreover, the potential tracer connected to the reference electrode constantly indicates the potential of the electrode which it is connected. Although, the control circuit adjusts this current to ensure that the potential between the reference electrode and the working electrode is equal to the output potential of the linear voltage generator, the measured potential is the potential between the work and the reference electrode. Finally, during the test run the working electrode is at the known true potential and this potential is recorded as a function of time (Erdoğan 2009).

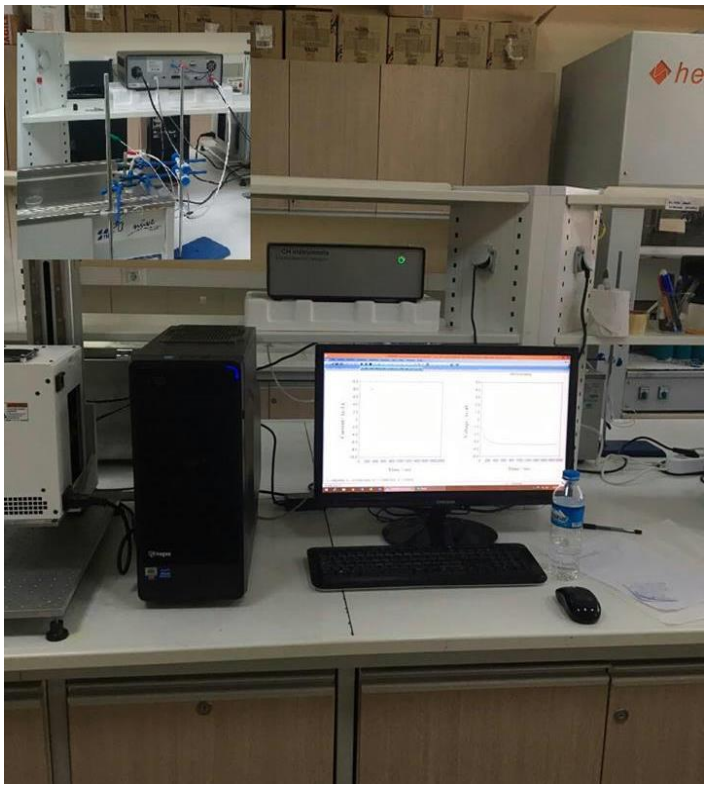

Figure 3.7. A photo of the potentiostat system used in our studies

Photoelectrochemical studies were carried out with a CHI electrochemical analyzer (CHI 6096 E Inc., USA) in a three-electrode configuration with, indium tin oxide (ITO) coated glass as working electrode, Platinum wire (Pt) as a counter electrode, Ag/AgCl and standard calomel electrode SCE as the reference electrode. In our studies we used (CHI 6096E USA) type operational potentiostat in our studies (Figure 3.7). It alternating voltammetry through potentiostat, potentially controlled electrolysis and amperimetric techniques were used for analysis.

3.2. The Used Methods

3.2.1. The Electrochemical Methods

Voltammetry, an electroanalytical method used in electrochemistry, on the condition that a working electrode is polarized so that information about the analyte can be obtained, (Skoog et al. 1998), in which the flow is measured in the form of a potential function to be applied. To provide the voltammeter polarization, the surface area of the working electrodes is taken to be a few millimeters square, and a few micrometers square (Heyrovsky 1922). Using mercury electrode as a microelectrode is the most important difference that separates polarography, a special type of voltammetry, from other voltammetric techniques. Voltammetry used for many analytical purposes, is widely used for non-analytical purposes. As an example, in the investigation of adsorption processes on the surface, examination of the oxidation / reduction processes occurring in various media, as elucidation of electron transfer mechanisms occurring on chemically modified electrode surfaces (Erdoğan 2009).

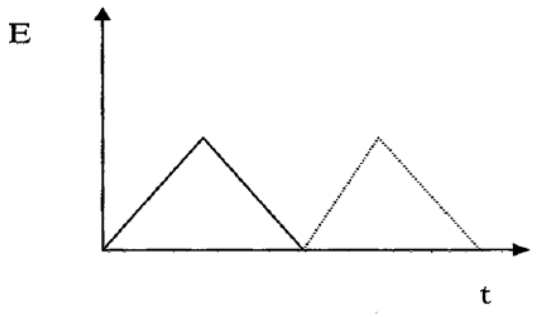

Figure 3.8. Cyclic voltammetric technique for conversion the potential vs time

The cyclic voltammetry is increased in potential linearly as a function of time up to a certain potential value and returned to its starting potential again as shown in (Figure 3.8).

The graphs of the potential versus current values obtained by using the alternating voltammetry technique are called voltamograms. Usually, electrochemical information is given in the form of these graphs (Malachesky 1969). Potential values and currents can be measured at the same time when the reaction occurs in an electrochemical cell. The potential of the working electrode is changed between the values determined in the negative and positive direction based on the potential of the reference electrode by means of a potentiostat. Electrode potential is scanned in the positive direction and a current is generated by the presence of molecules or ions in the environment reaching the oxidation potential. This flow is called the anodic current. If the electrode is to be scanned on a potentially negative side, a current will be generated due to the reduction of the electroactive substances when the ions or molecules in the environment reach the reduction potential, and the generated current is called the cathodic current (Skoog et al. 1998).

For a cyclic electrode response, there must be a voltage difference between the cathodic peak potential (Epc) and the anodic peak potential (Epa) (0.059/n) V. The formal potential (E^o) of the redox couple examined is equal to the midpoint of these two peak potentials. For an alternating voltamogram, the ratio of anodic peak current to cathodic peak current is approximately one ($I_{pa} / I_{pc} \cong 1$).

$$Ox + ne^- \leftrightarrow Red \qquad (3.2)$$

For Equation 3.2, the amount of oxidant on the surface decreases with time, so the current will fall and the reaction will end. Thus, a selective reaction will be realized by adjusting potential. The reference electrode is used in addition to the working electrode and the counter electrode. According to the Nernst equation, as the concentrations of the electroactive substances change with time, the potential of the working electrode is always kept constant by using the potentiostat.

According to the Nernst equation (Equation 3.3) for Equation 3.2, the concentration of oxidant will decrease over time and will potentially change with time. The oxidant in the environment, it will remain at fixed value for the potential short-term with the exhaustion of the whole (Erdoğan 2009).

$$E = E^{o} - \frac{RT}{nF} \ln \frac{[Red]}{[Ox]} \tag{3.3}$$

E_{cell} is the cell potential,

E°cell is the standard cell potential,

R is the universal gas constant: R = 8.314472(15) J K^{-1} mol^{-1},

n is the number of moles of electrons transferred in the cell reaction or half-reaction,

F is Faraday constant, the number of coulombs per mole of electrons,

F = 9.64853399(24)×10^{4} C mol^{-1},

T is the temperature in kelvins at room temperature (25 °C),

RT/F may be treated like a constant and replaced by 25.693 mV for cells.

3.2.2. UV-VIS Spectroscopy

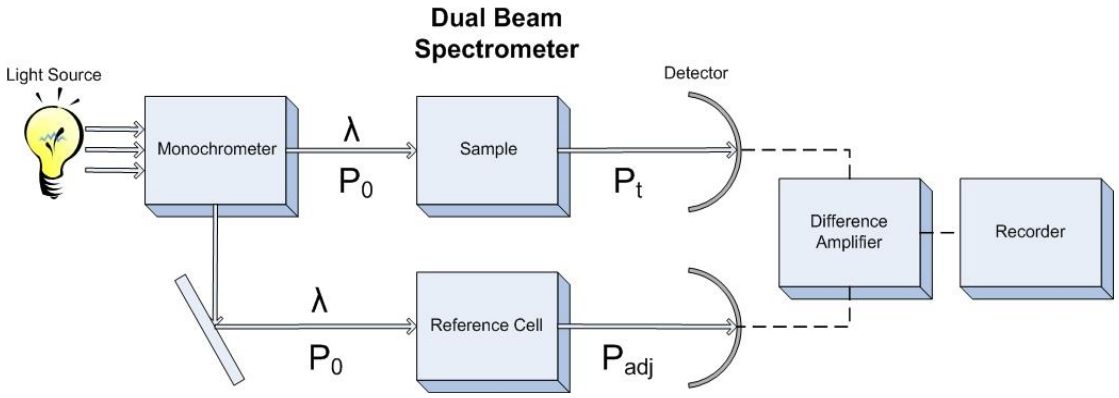

Figure 3.9. Schematically representation of double beam spectrometer

Molecular absorption spectroscopy is the method of measuring the absorbance (A) or permeability (T) of a solution in a cell by using the wavelengths. Absorption in the ultraviolet and visible region is mainly due to the stimulation of the bonding electrons in

the molecules. As a result, the wave lengths of the absorption peaks with the types of bonds in the species studied and are thus used in the quantitative determination of functional groups in a molecule as well as of compounds carrying functional groups (URL-2 2015). The components of the double-light-path spectrometry are shown in Figure 3.9.

The components of the double-light-path spectrometry are shown in Figure 3.9. In the first the light comes from the light source to a monochromator. And then the light from the monochromator is sent to the reference and sample cells, separated by two equal wavelengths. These two light beams sent to the sample cell and reference cell are detected with two different detectors. Finally, the permeability value of the reference cell and the permeability value of the sample cell are continuously compared in the signal readout, and the ratio of the generated signals is read. The spectrophotometer used in our studies is shown in Figure 3.10.

Figure 3.10. Shimadzu UV-3600 UV-VIS-NIR spectrophotometer used in our studies

3.2.3. SEM

Scanning Electron Microscopy (SEM) is a powerful method for the investigation of surface structures of Molecules, this technique provides a large depth of field, which means, and the area of the sample that can be viewed in focus at the same time is actually

quite large. SEM has also the advantage that the range of magnification is relatively wide allowing the investigator to easily focus in on an area of interest on a sample that was initially scanned at a lower magnification. Furthermore, the three-dimensional appearing images may be more appealing to the human eye than the two-dimensional images obtained with a transmission electron microscope. Therefore, an investigator may find it easier to interpret SEM images. Finally, the number of steps involved for preparing specimens for SEM investigation is lower and thus the entire process is less time consuming than the preparation of samples for investigation with a transmission electron microscope.

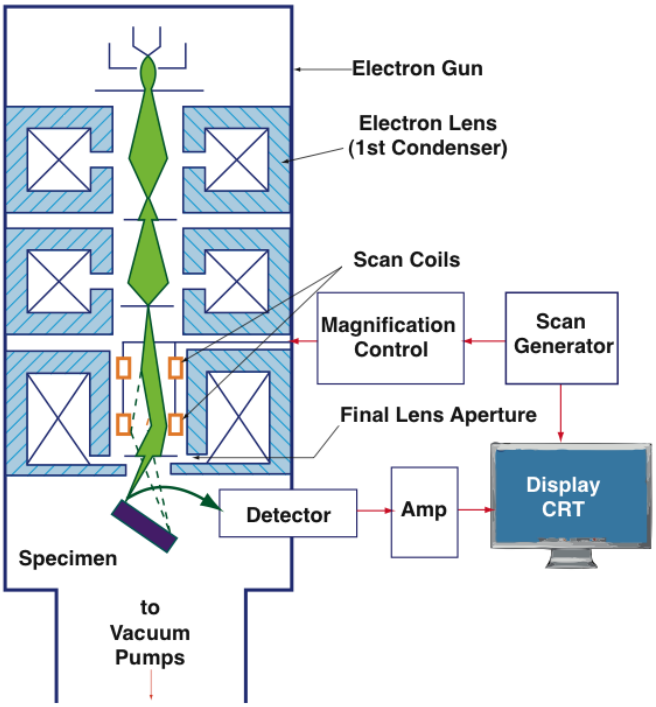

Figure 3.11. Schematically representation the main components of SEM column scanning system

Essential components of all SEMs include electron column, scanning system, detector, display, vacuum system and electronics controls. Infrastructure requirements: rower supply, vacuum system, cooling system beam condenser, vibration-free floor, room free of ambient magnetic and electric fields. SEMs always have at least one detector (usually a secondary electron detector), and also most have additional detectors as shown in (Figure 3.11). The electron column of the SEM consists of an electron gun and two or more electromagnetic lenses operating in vacuum. The electron gun generates free

electrons and accelerates these electrons to energies in the range 1-40 Kev in the SEM. The purpose of the electron lenses is to create a small focused electron probe on the sample. Most SEMs can generate an electron beam at the specimen surface with spot size less than 10 nm in diameter while still carrying sufficient current to form acceptable image. Typically, the electron beam is defined by probe diameter in the range of 1 nm to 1 μm. In order to produce images, the electron beam is focused into a fine probe, which is scanned across the surface of the sample with the help of scanning coils. Moreover, each point on the specimen that is struck by the accelerated electrons emits signal in the form of electromagnetic radiation. Selected portions of this radiation, usually secondary or backscattered electrons are collected by a detector and the resulting signal is amplified and displayed on a computer screen or computer monitor.

The SEM has a large depth of field about 30 mm, which allows a large amount of the sample to be in focus at the same time and produce an image that is a good representation of the three-dimensional sample. In addition, the combination of higher magnification, large depth of field, greater resolution, commotional and crystallographic information makes the SEM one of the most highly used in lab searches area and industry. A SEM may be equipped with an EDX analysis system to enable it to perform compositional analysis on specimens. EDX analysis is useful in identifying materials and contaminants, as well as estimating their relative concentrations on the surface of the specimen (Stadtlander 2007).

3.2.4. EDX

Energy-dispersive X-ray spectroscopy (EDX) is a type of spectroscopy used by SEM to provide information on the chemical composition of the sample being examined in the SEM (Figure 3.12). Compared to other spectroscopic techniques used for the same purpose, it is quite advantageous. In EDX, when the electron beam transmitted to the sample interacts with the atoms of the sample, the energy is around 10-20 keV, causing X-ray photons to spread through the sample. Detection of these emitted photons is carried out by means of an energy separation spectrometer. EDX is based on the principle that the produced x-rays are measured as a function of the energy, and the chemical composition of the sample to be examined is determined according to the properties of

the X-rays emitted from the sample. The portion of the sample to be analyzed may be the entire sample, a region, or any point. Thus, chemical analysis of any desired region during image acquisition can be performed. The energy of x-ray photons generated by sending an electron beam depends on the characteristics of the sample under investigation. As the emitted electrons form x-rays in the inner regions rather than the sample surface, EDX does not give information about the surface properties. In addition, Also, it is not very useful to use it in EDX analyzes because the X-ray intensity of elements with low atomic number is low. The fact that the EDX analysis can be performed at the same time as the acquisition of the SEM image, and the analysis without making the sample dissolve by any means, is a significant advantage of EDX (URL-3-4 2016). The EDX system used in our studies (JEOL JSM-6510) shown in Figure 3.12.

Figure 3.12. The EDX and SEM system we use in our studies (JEOL JSM-6510)

3.2.5. XRD

The X-ray diffraction method is widely used in the determination of crystal structures. XRD devices have improved significantly after the Fourier Transform revolution. Sharp wide angle, short time and suitable output devices were analyzing each angle individually prior to offering a collective value. The ability to collect fingerprint sensitive data in crystal structures makes XRD very useful and reliable. The XRD Crystal is a technique

that can determine the distance between atomic planes. The working principle is based on the collection of scatter and diffraction data by sending and scanning the x-ray to the sample to be analyzed. The X-rays are sent to a crystal plane and reflected by the crystal plane of the atoms, which is an X-ray diffraction phenomenon. This actual reflection is different from the reflection of the light from a mirror plane. Diffraction is not a superficial phenomenon. In other words, incoming x-rays reach the plane of the atoms beneath the crystal surface.

Wavelength fixed X-rays are used in XRD studies. To obtain these x-rays, electrons emitted by heating a filament, such as tungsten, is accelerated in the field and accelerated to an electron beam which is energized with high energy. These electrons reach the anodic electron shells (Skoog et al. 1998). If the electron beam collides with an electron in the shell near the core, the electron is removed from its position and the atom becomes unstable due to electron loss. When If the vacant electron fills an electron in the higher energy crust shell, an energy difference occurs due to this electron transition, and this energy difference is spread as a photon of X-rays. The XRD device used in our studies is shown in Figure 3.13.

Figure 3.13. The XRD device (Rigaku Ultima IV)

A way in which the rays reflected by the atomic planes collide with the X-ray beam at a certain angle, known as the Bragg angle, which is equal to the exact multiple of the wavelength (λ), the rays will have the same phase and the diffraction will occur come to a point. It is shown in Figure 3.14, to obtain the diffraction peak; It is necessary to have a relation between the angle of attack (θ) of the x-rays to the atomic planes, the distance (d) between the atomic planes and the wavelength λ of the incoming X-rays, the difference between the lengths of the paths that X-rays take it (Erdoğan 2009).

X-ray diffraction is a powerful tool to study the crystal structure of semiconductors. XRD gives information about crystalline phase, quality, orientation, composition, lattice parameters, defects, stress, and strain of samples. Every crystalline solid has its unique characteristic X-ray diffraction pattern, which is identified by this unique ‘‘fingerprint’’. Crystals are regular arrays of atoms and they are arranged in a way that a series of parallel planes separated from one another by a distance d. Figure 3.14 shows the detail of the process of x-ray diffraction. If an x-ray beam with a wavelength strikes the sample with an incident angle, then the scattered ray is determined by Bragg’s law (n = 2dsin). Where n is an integer, is the wavelength of the beam, d is the spacing between diffracting planes, and is the incident angle of the beam. The set of d-spacing in a typical x-ray scan provides a unique characteristic of the samples in question (Amin and Willander 2012).

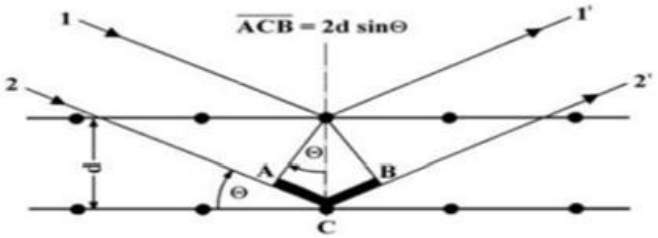

Figure 3.14. Schematic diagram of Bragg's reflection from lattice planes in a crystalline structure with by development of X-ray diffraction

$$ACB = AC + CB \tag{3.4}$$

$$\sin\theta = AC / d = CB / d \tag{3.5}$$

$$AC = CB = d \sin\theta \tag{3.6}$$

The difference between the lengths of the paths of the X-rays is given by Equation 3.7 below.

$$AC + CB = 2d \sin\theta \quad (3.7)$$

$$ACB = 2d \sin\theta \quad (3.8)$$

In order for the diffraction to be possible, this path difference must be equal to the multiple of λ or λ. Thus Equation 3.8 can be written (Erdoğan 2009).

$$ACB = n\lambda \quad (3.9)$$

$$2d \sin\theta = n\lambda \quad (3.10)$$

3.2.6. Photoelectrochemical System

The photoelectrocatalytic performances of these oxides formed on ITO coated glass electrodes were measured under sunlight, which is represented by a three-electrode system (Figure 3.15). The photoelectrochemical measurements were recorded under a beam of AM 1.5G using a Solar Light-16S-002 brand solar simulator with a 150 W xenon arc lamp. The photocurrent-potential, and photocurrent-time curves were measured using linear sweep voltammetry and chronoamperometry techniques, respectively.

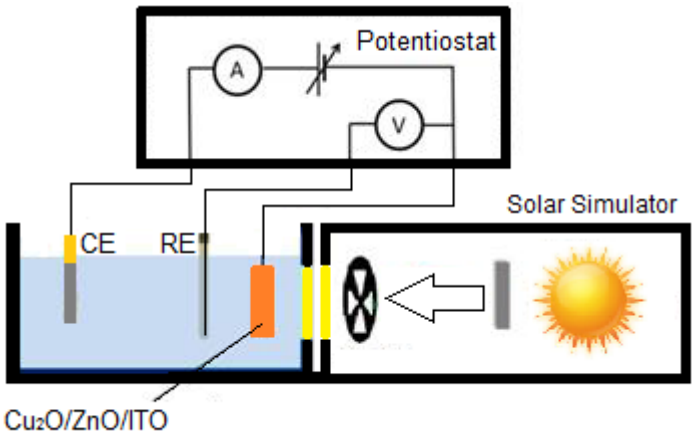

Figure 3.15. Schematic representation of the instrument used for photoelectrochemical measurements

4. FINDINGS AND DISCUSSION

4.1. Electrochemical Studies

In this thesis study, it was reported on the synthesis of homogeneous Cu_2O photoelectrodes with various deposition times using UPD based electrochemical technique. In principle, UPD, the electrochemical deposition of a metal onto a substrate at potentials more positive than the Nernst potential, is usually restricted to the formation of one atomic layer of the deposited metal. Therefore, in order to deposit an atom at a time, very small amounts of dissolved copper and oxygen species are needed in the solution phase for deposition at UPD. The UPD potential for copper was determined by cyclic voltammetric measurements. In order to determine a deposition potential of the copper (I) oxide from the solution, the cyclic voltammetric measurements of copper were also recorded at the UPD region in the aqueous medium. The results showed that the bulk Cu deposition does not occur until −200 mV. If the potential of the working electrode is kept constant at a more positive potential than −200 mV, copper and oxygen are supposed to deposit underpotentially at the ITO coated electrode surface. These electrodeposited Cu and O react to form the Cu_2O semiconductor on ITO coated surface. The amount of electrodeposited Cu_2O will depend on the deposition time. Thus, electrodepositions of Cu_2O nanostructrures with various dimensions on ITO coated electrode surface could be achieved by this method using different deposition times.

4.2. XRD Studies

Figure 4.1 is XRD diffractograms of Cu_2O photoelectrodes electrodeposited for 15 min. The XRD diffractogram of copper (I) oxide consists of a strong diffraction peak at 36.6° arising from (1 1 1) reflections from Cu_2O. The weaker diffractions at 42.5°, 61.7°, and 73.9° corresponds to (2 0 0), (2 2 0), and (3 1 1) reflections of Cu_2O. The other peaks belong to ITO coated glass which belongs to working electrode in this study. The other

XRD diffractograms of Cu_2O at different deposition times are similar to Figure 4.1. As the deposition time is increased, the intensity of Cu_2O diffractions increases. These XRD results indicate that highly crystalline materials of Cu_2O.

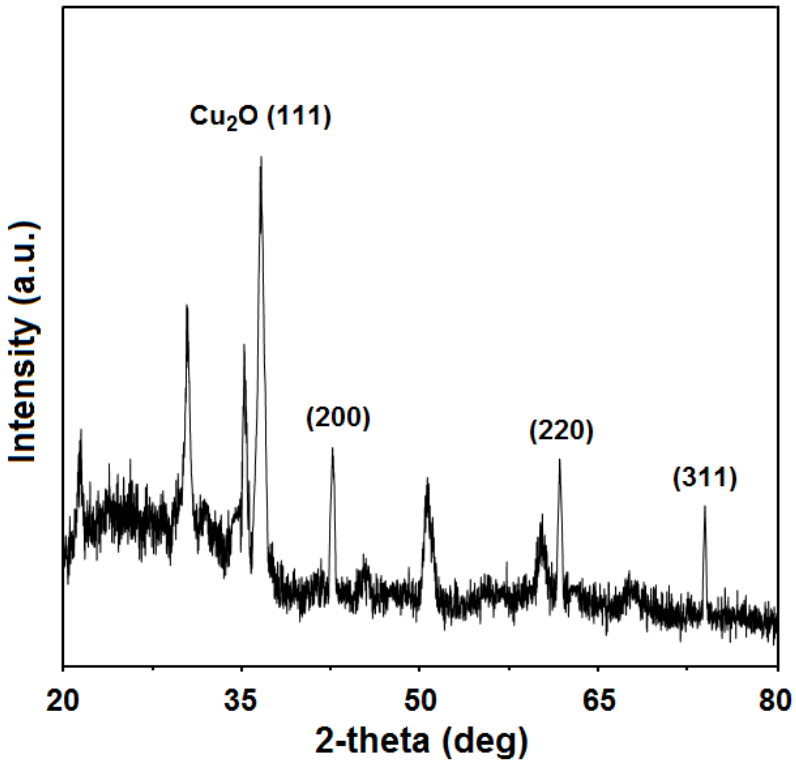

Figure 4.1. The XRD diffractogram of Cu_2O photoelectrodes electrodeposited for 15 min

4.3. SEM and EDX Studies

Figure 4.2 shows SEM image of ITO coated glass surface which belongs to working electrode in this study. Figure 4.3 shows a SEM image obtained after electrodeposition of Cu_2O semiconductor material on ITO coated glass for 15 min. Evenly distributed Cu_2O nanocubes of approximately the same size are observed on the surface of the ITO coated electrode. Most Cu_2O semiconductor nanocubes have a uniform shape. The average sizes of Cu_2O semiconductor nanocubes observed for 15 min were about 250 nm in diameter. The other SEM images of Cu_2O at different deposition times are similar to Figure 4.3. As the electrodeposition time increases, Cu_2O nanocubes diameters increase.

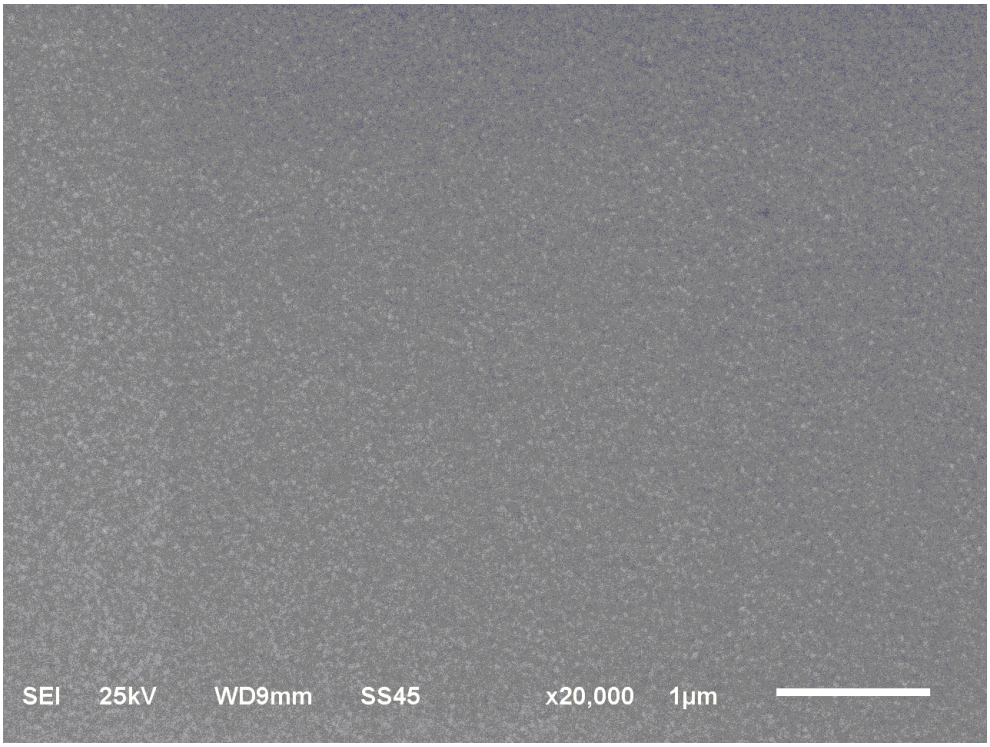

Figure 4.2. SEM image of ITO coated glass working electrode

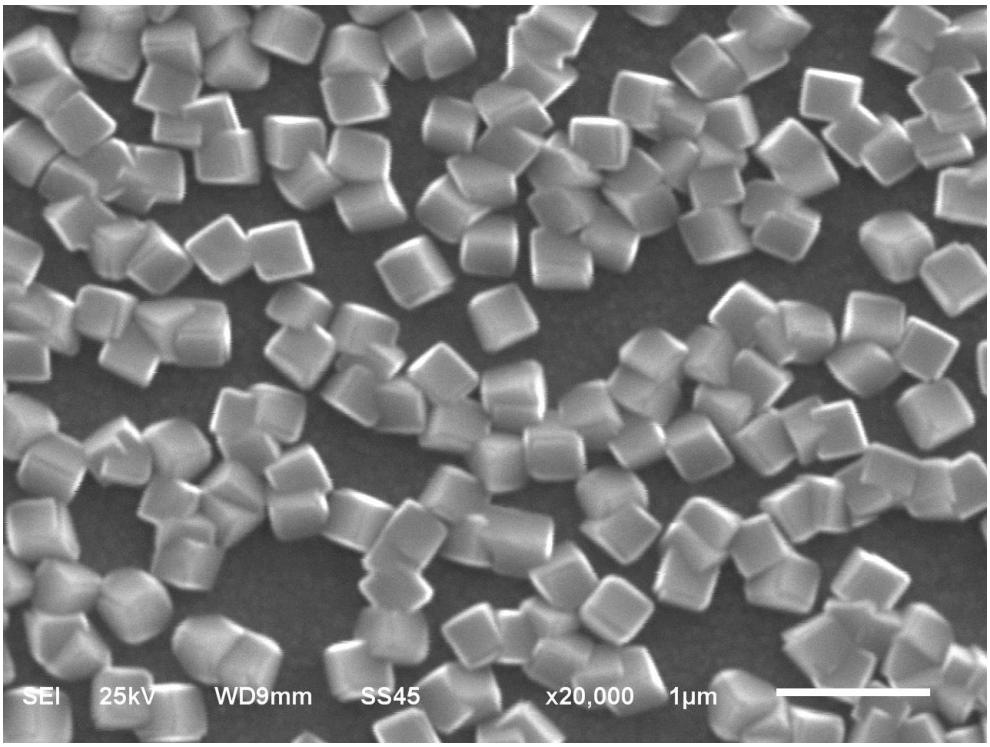

Figure 4.3. SEM image of Cu_2O photoelectrodes electrodeposited onto ITO coated glass surface

The elemental compositions of the Cu_2O semiconductor photoelectrodes were determined by the EDX. The absence of any other peaks indicates that the Cu_2O are homogeneous in composition and formed from Cu-O. EDX analyses of different regions gave the same results. For the copper (I) oxide semiconductors, the quantitative atomic ratios of Cu/O are close to 1/2 stoichiometry.

4.4. Absorbance and Band Gap Studies

Absorbance spectrum of Cu_2O semiconductor photoelectrodes electrodeposited for 15 min is shown in Figure 4.4. In here, one absorption band in the UV-Vis region observed. The absorption edge measured for photoelectrodes are 585 nm. The fundamental absorption edges at 585 nm correspond to Cu_2O. The other absorbance spectrums of Cu_2O semiconductor photoelectrodes at different deposition times are similar to Figure 4.4.

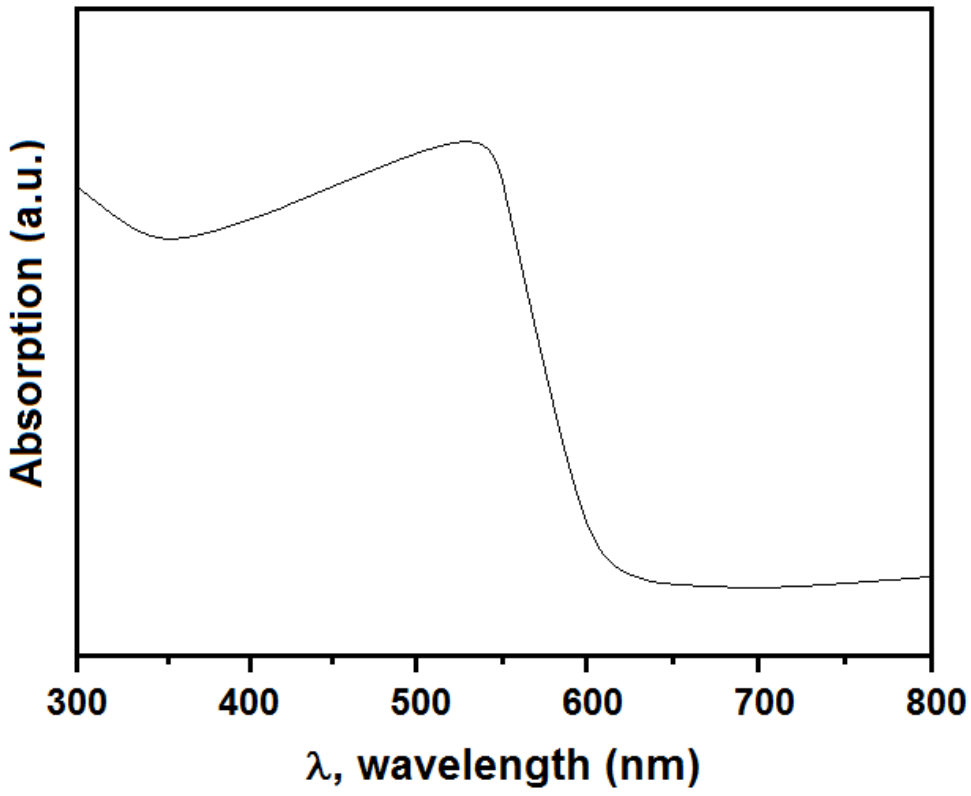

Figure 4.4. Absorbance spectrum of Cu_2O semiconductor photoelectrodes electrodeposited for 15 min

For all the semiconductors, the widely used method of plotting $(\alpha hv)^2$ versus the energy hv is adopted to determine the band gap of the materials. The Eg can thus be estimated from a plot of $(\alpha hv)^2$ versus the photon energy hv. The band gap of Cu_2O semiconductors electrodeposited onto ITO coated glass was found to be Eg = 2.12 eV.

4.5. PEC Studies

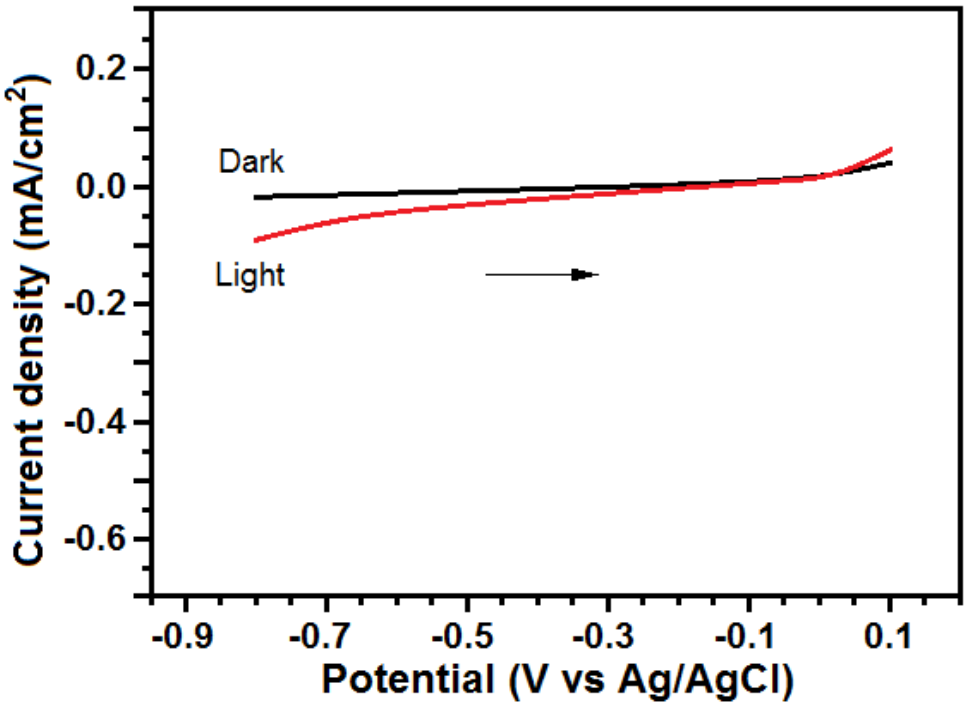

Figure 4.5. Linear sweep voltammograms of Cu_2O semiconductor photoelectrodes electrodeposited for 1 min in 0.1 M Na_2SO_4

Figure 4.5-13 shows the effect of electrochemical deposition time on the light and dark currents of Cu_2O semiconductor photoelectrodes. Figure 4.5 shows linear sweep voltammograms of Cu_2O semiconductor photoelectrodes electrodeposited for 1 min in dark and light. This linear sweep voltammogram exhibited a photocathodic behavior due to the p-type nature of the Cu_2O semiconductors.

Figure 4.6 shows linear sweep voltammograms of Cu_2O photoelectrodes electrodeposited for 3 min. It also exhibited a photocathodic behavior. The photocurrents increased with longer deposition time.

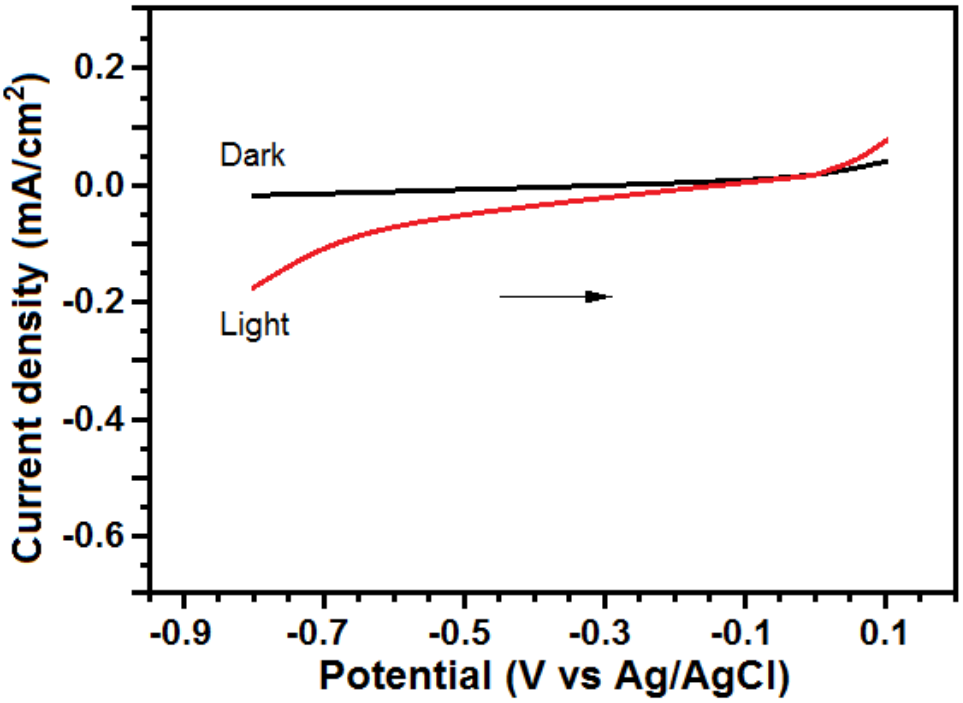

Figure 4.6. Linear sweep voltammograms of Cu_2O semiconductor photoelectrodes electrodeposited for 3 min in 0.1 M Na_2SO_4

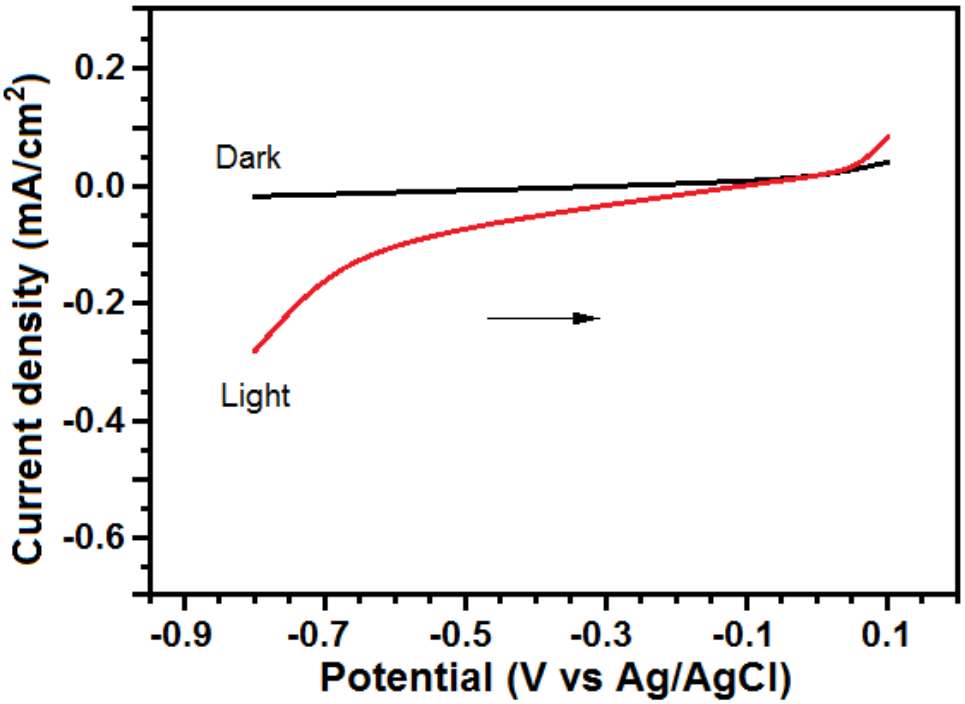

Figure 4.7. Linear sweep voltammograms of Cu_2O semiconductor photoelectrodes electrodeposited for 5 min in 0.1 M Na_2SO_4

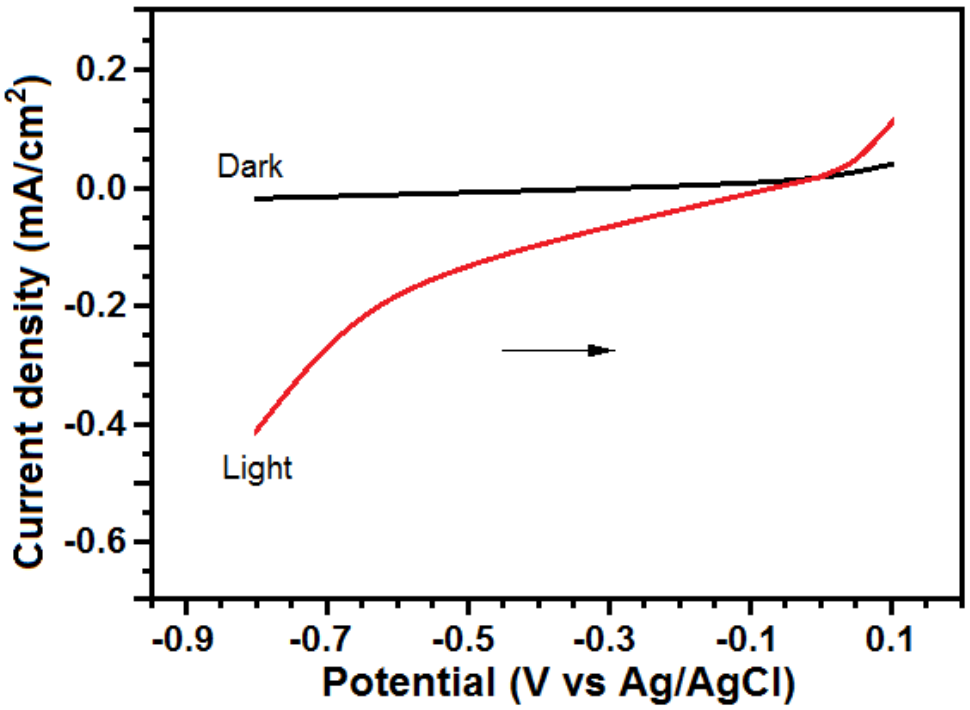

Figure 4.8. Linear sweep voltammograms of Cu_2O semiconductor photoelectrodes electrodeposited for 10 min in 0.1 M Na_2SO_4

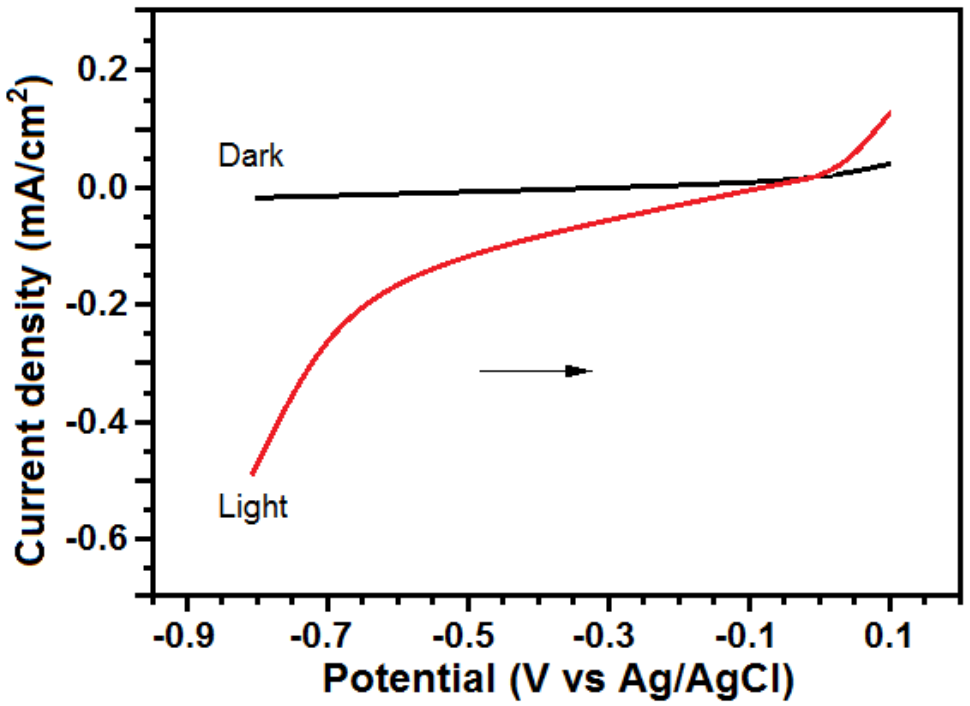

Figure 4.9. Linear sweep voltammograms of Cu_2O semiconductor photoelectrodes electrodeposited for 15 min in 0.1 M Na_2SO_4

Figure 4.7,8 and 9 exhibit linear sweep voltammograms of Cu_2O semiconductor photoelectrodes for 5, 10 and 15 min, respectively. As the electrochemical deposition time increased, the photocurrents of Cu_2O semiconductor photoelectrodes increased. The Cu_2O semiconductor photoelectrodes electrodeposited for 15 min exhibit the highest photocurrents between the investigated all semiconductor films.

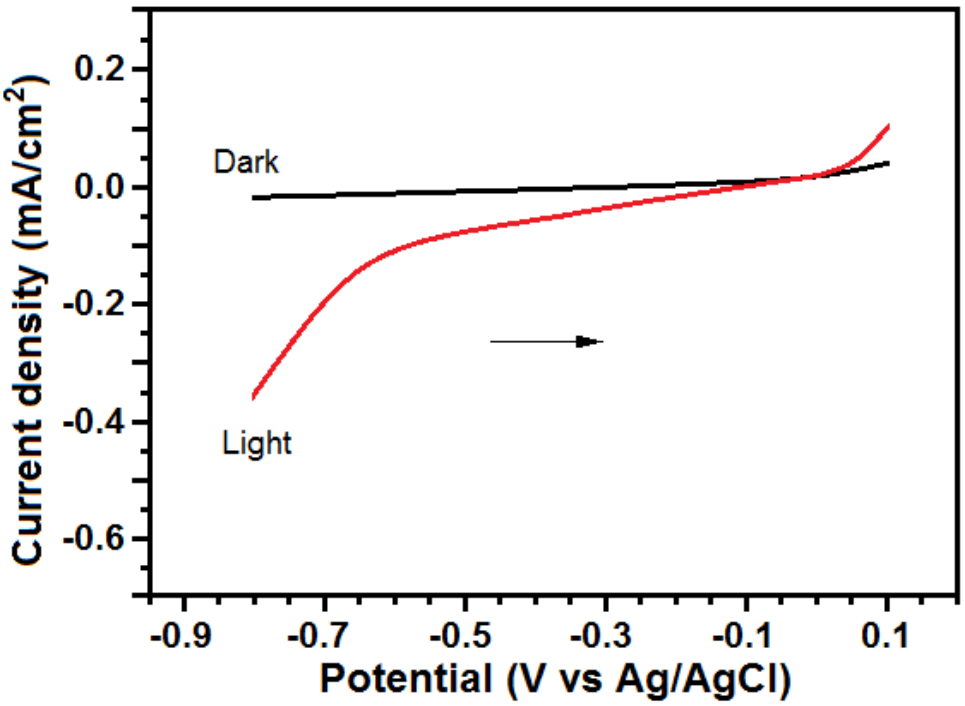

Figure 4.10. Linear sweep voltammograms of Cu_2O semiconductor photoelectrodes electrodeposited for 30 min in 0.1 M Na_2SO_4

Figure 4.10, 11, 12 and 13 exhibit linear sweep voltammograms of Cu_2O semiconductor photoelectrodes for 30, 60, 120 and 180 min, respectively. As the electrochemical deposition time increased, the photocurrents of Cu_2O semiconductor photoelectrodes decreased. After 120 min, the photocurrents of Cu_2O semiconductor photoelectrodes remained almost constant. This may be due to the increased bending of Cu_2O semiconductor photoelectrodes for higher deposition times, which may reduce the effective area for surface reactions leading to lower photocurrents. All the linear sweep voltammograms showed a photocathodic behavior due to the p-type nature of the Cu_2O semiconductors.

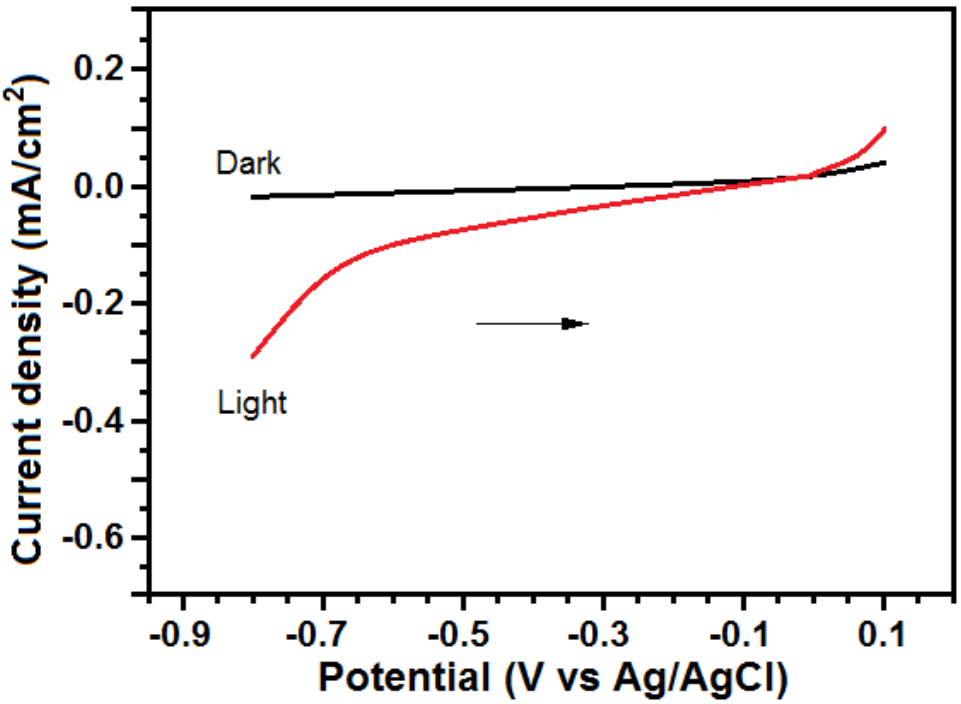

Figure 4.11. Linear sweep voltammograms of Cu_2O semiconductor photoelectrodes electrodeposited for 60 min in 0.1 M Na_2SO_4

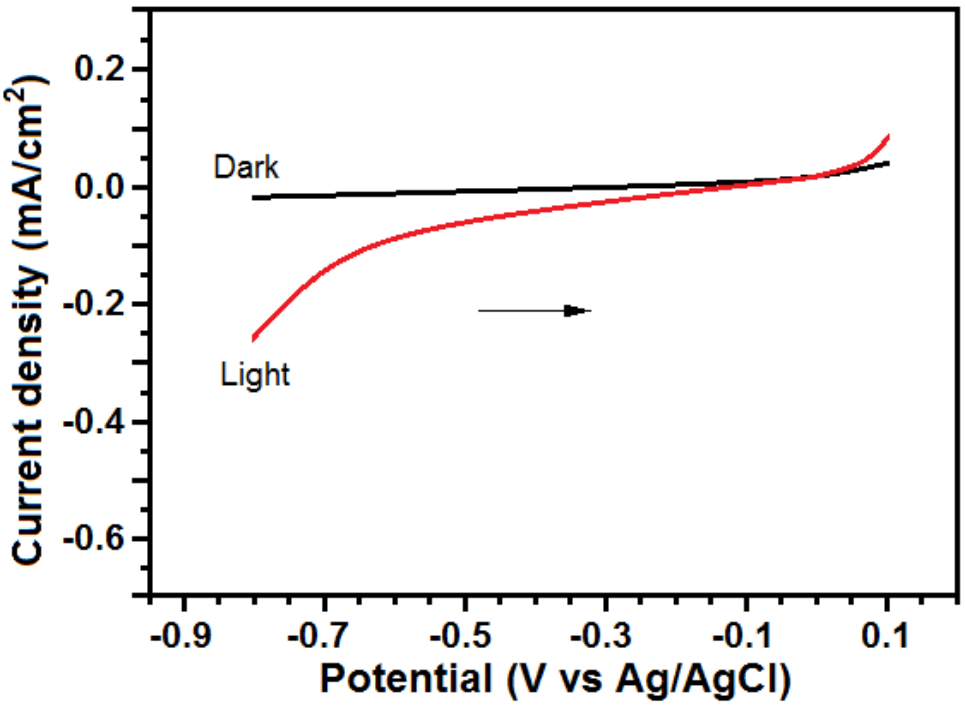

Figure 4.12. Linear sweep voltammograms of Cu_2O semiconductor photoelectrodes electrodeposited for 120 min in 0.1 M Na_2SO_4

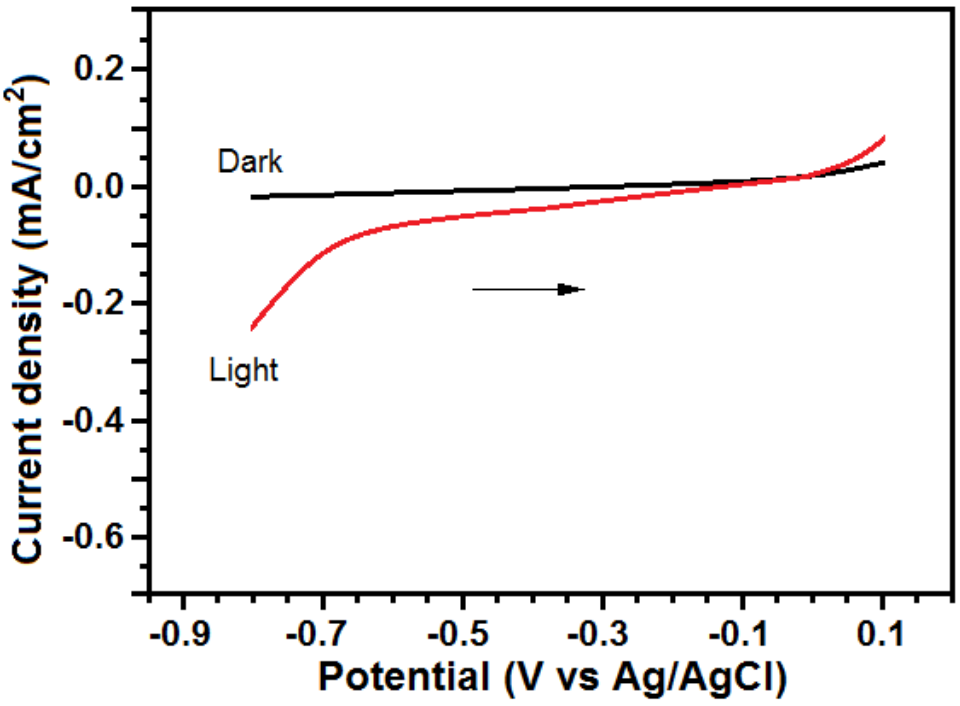

Figure 4.13. Linear sweep voltammograms of Cu_2O semiconductor photoelectrodes electrodeposited for 180 min in 0.1 M Na_2SO_4

Figure 4.14 illustrates the current density under sun light for the corresponding copper (I) oxide semiconductor photoelectrodes. Herein, the effect of Cu_2O electrodeposition time on the photocurrents of photoactive films is exhibited.

Figure 4.14.a shows chronoamperogram of Cu_2O semiconductor photoelectrodes electrodeposited for 1 min under light. Figure 4.14.b, c, d and e exhibit chronoamperograms of Cu_2O semiconductor photoelectrodes for 3, 5, 10 and 15 min, respectively. As the electrochemical deposition time increased, the current density of Cu_2O semiconductor photoelectrodes increased. The Cu_2O semiconductor photoelectrodes electrodeposited for 15 min (Figure 4.14.e) exhibit the highest current density between the investigated all semiconductor films. Figure 4.14.f, g, h, and i show chronoamperograms of Cu_2O photoelectrodes for 30, 60, 120 and 180 min, respectively. As the electrochemical deposition time increased, the current density of Cu_2O semiconductor photoelectrodes decreased. After 120 min, the current density of Cu_2O semiconductor photoelectrodes remained almost constant.

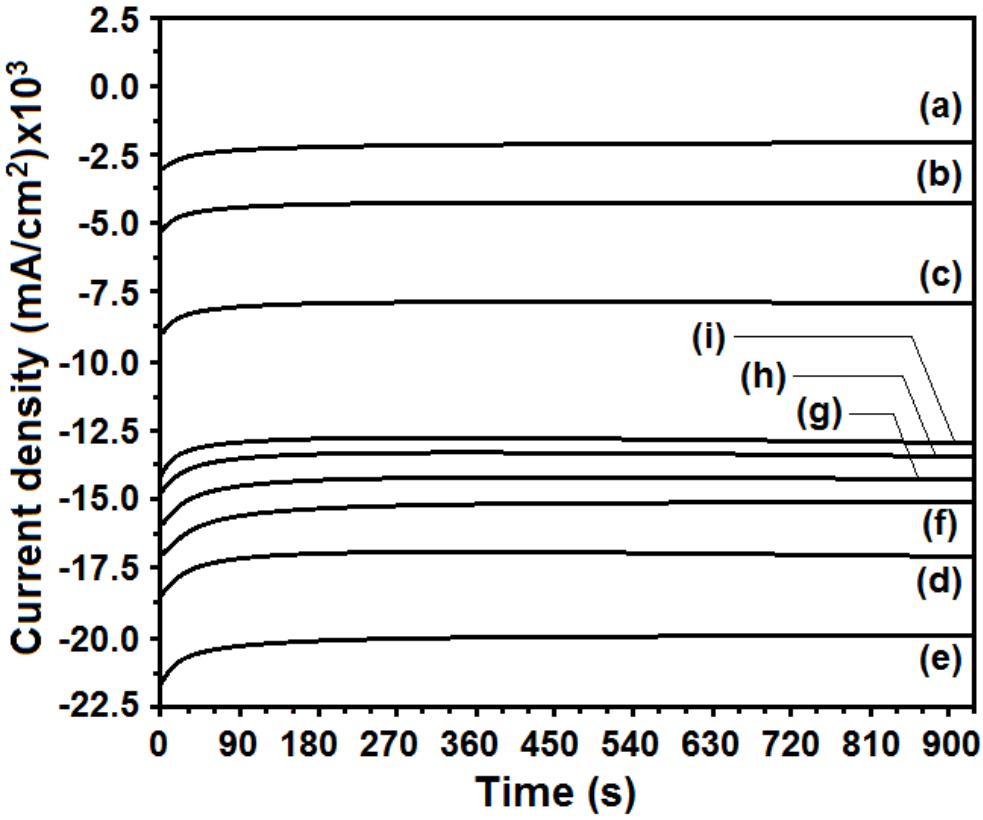

Figure 4.14. Photocurrent responses of Cu_2O semiconductor photoelectrodes under light illumination in 0.1 M Na_2SO_4. Current density of copper (I) oxide photoelectrodes electrodeposited for (a) 1, (b) 3, (c) 5, (d) 10, (e) 15, (f) 30, (g) 60, (h) 120, and (i) 180 min

The trends for different electrodeposition times in the current density (Figure 4.14) confirm the observed trends in Figure 4.5-13. As shown in Figure 4.14, Cu_2O photoelectrodes exhibit good stability and switching behavior for different Cu_2O electrodeposition times.

5. RESULTS AND RECOMMENDATIONS

This study reports on the synthesis of homogeneous Cu_2O photoelectrodes with various deposition times using UPD based electrochemical technique. The UPD potential for copper was determined by cyclic voltammetric measurements. In order to determine a deposition potential of the copper (I) oxide from the solution, the cyclic voltammetric measurements of copper were also recorded at the UPD region in the aqueous medium. These electrodeposited Cu and O react to form the Cu_2O semiconductor on ITO coated surface. The amount of electrodeposited Cu_2O will depend on the deposition time. Thus, electrodepositions of Cu_2O nanostructrures with various dimensions on ITO coated electrode surface could be achieved by this method using different deposition times.

The XRD diffractograms of copper (I) oxide consists of a strong diffraction peak arising from (1 1 1) reflections from Cu_2O. The weaker diffractions corresponds to (2 0 0), (2 2 0), and (3 1 1) reflections of Cu_2O. As the deposition time is increased, the intensity of Cu_2O diffractions increases. These XRD results indicate that highly crystalline materials of Cu_2O.

In SEM images, evenly distributed Cu_2O nanocubes of approximately the same size are observed on the surface of the ITO coated electrode. Most Cu_2O semiconductor nanocubes have a uniform shape. As the electrodeposition time increases, Cu_2O nanocubes diameters increase. The EDX analyses indicate that the Cu_2O are homogeneous in composition and formed from Cu-O. EDX analyses of different regions gave the same results. For the copper (I) oxide semiconductors, the quantitative atomic ratios of Cu/O are close to 1/2 stoichiometry.

The absorption edge measured for photoelectrodes are 585 nm. The fundamental absorption edges at 585 nm correspond to Cu_2O. The Eg can thus be estimated from a

plot of $(\alpha hv)^2$ versus the photon energy hv. The band gap of Cu_2O semiconductors electrodeposited onto ITO coated glass was found to be Eg = 2.12 eV.

The Cu_2O semiconductor photoelectrodes electrodeposited for 15 min exhibit the highest photocurrents and the current density between the investigated all semiconductor films. After 120 min, the photocurrents and the current density of Cu_2O semiconductor photoelectrodes remained almost constant. This may be due to the increased bending of Cu_2O semiconductor photoelectrodes for higher deposition times, which may reduce the effective area for surface reactions leading to lower photocurrents. All the linear sweep voltammograms showed a photocathodic behavior due to the p-type nature of the Cu_2O semiconductors. Cu_2O photoelectrodes exhibit good stability and switching behavior for different Cu_2O electrodeposition times. Cu_2O semiconductor photoelectrodes are suggested as a competitive candidate for advanced photoelectrochemical detection, maybe for the extended field of photoelectrochemical water splitting and other solar photovoltaic technologies.

REFERENCES

Abdellah M, Thomas JP, Zhang L, Tong K (2016) Solar Cells Enhancement of solar cell performance of p-Cu_2O/n-ZnO-nanotube and nanorod heterojunction devices. Solar Energy Materials and Solar Cells 152: 87–93.

Alkoy EM, Kelly JM (2005) The structure and properties of copper oxide and copper aliminium oxide coating prepared by pulsed magnetron sputtering of powder targets. Vacuum 79: 221–230.

Aranda PR, Pacheco PH, Olsina RA, Martinez LD, Gil RA (2009) Total and inorganic mercury determination in biodiesel by emulsion sample introduction and FI-CVAFS after multivariate optimization, J. Anal. At. Spectrom. 24: 1441–1445.

Bartlett PN, Baumberg JJ, Coyle S, Abdelsalam ME (2004) Optical properties of nanostructured metal films. Faraday Discussions 125: 117–132.

Chang SJ, Hsueh TJ, Hsueh HT, Hung FY, Tsai TY, Weng WY, Hsu CL, Dai BT (2011) CuO nanowire-based humidity sensors prepared on glass substrate. Sensors and Actuators B: Chemical 156: 906–911.

Dolui SK, Phukon P, Nath BC, Das D (2013) Synthesis and evaluation of antioxidant and antibacterial behavior of CuO nanoparticles. Colloids and Surfaces B: Biointerfaces 101: 430–433.

Feng X, Guo C, Mao L, Ning J, Hu Y (2014) Facile growth of Cu_2O nanowires on reduced graphene sheets with high nonenzymaticelectrocatalytic activity toward glucose. Journal of the American Ceramic Society 97(3): 811–815.

Fung KZ, Liao CL, Chang ST, Leu IC, Lee YH (2004) The electrochemical capacities and cycle retention of electrochemically deposited Cu_2O thin film toward lithium. Electrochimica Acta 50: 553–559.

Gunasekaran S, Zhang WD, Jiang LC, Yang J (2010) A highly sensitive non-enzymatic glucose sensor based on a simple two-step electrodeposition of cupric oxide (CuO) nanoparticles onto multi-walled carbon nanotube arrays. Talanta 82: 25–33.

Jayathileke KMDC, Siripala W, Jayanettib JKDS (2008) Electrodeposition of p-type, ntype and p-n Homojunction Cuprous Oxide Thin Films. Sri Lanka Journal of Physics 9: 35–39.

Kandjani AE, Sabri YM, Periasamy SR, Zohora N, Amin MH, Nafady A, Bhargava SK (2015) Controlling core/shell formation of nanocubic p-Cu_2O/n-ZnO toward enhanced photocatalytic performance. Langmuir 31(39): 10922–10930.

Lee DS, Park KH, Park JW, Jung MY, Kang H, Choi NJ, Park HJ (2014) A ppb level formaldehyde gas sensor based on CuO nanocubes prepared using a polyol process. Sensors and Actuators B: Chemical 203: 282–288.

Li J, Li H, Xue Y, Fang H, Wang W (2014) Facile electrodeposition of environment friendly Cu_2O/ZnO heterojunction for robust photoelectrochemicalbiosensing. Sensors and Actuators B Chemical 191: 619–624.

Li F, Fan G (2011) Effect of sodium borohydride on growth process of controlled flowerlike nanostructured Cu_2O/CuO films and their hydrophobic property. Chemical Engineering Journal, 167: 388–396.

Liu XW, Wang FY, Zhen F, Huang JR (2012) In situ growth of Au nanoparticles on the surfaces of Cu_2O nanocubes for chemical sensors with enhanced performance. RSC Advances 2(20): 7647–7651.

Mahalingam T, Chitra JSP, Chu JP, Velumani S, Sebastian PJ (2005) Structural and annealing studies of potentiostatically deposited Cu_2O thin films. Solar Energy Materials and Solar Cells 88: 209–216.

Mathew X, Mathews NR, Sebastian PJ (2011) Temperature dependence of the optical transitions in electrodeposited Cu_2O thin films. Solar Energy Materials and Solar Cells 70: 277–286.

Mehta VK (2008) Principles of Electronics. S. Chand. p. 56.

Mukherjee N, Mondal A, Khan GG, Mitra BC, Bhar SK, Madhu U, Maji SK, Show B (2011) CuO nano-whiskers: Electrodeposition, Raman analysis, photoluminescence study and photocatalytic activity. Materials Letters, 65: 3248–3250.

Naskar MK, Roy M, Ghosh S (2014) Template-free synthesis of mesoporous singlecrystal CuO particles with dumbbell-shaped morphology. Materials Letters, 132: 98–101.

Pan Y, Deng S, Polavarapu L, Gao N, Yuan P, Sow CH, Xu QH (2012) Plasmon-enhanced photocatalytic properties of Cu_2O nanowire-Au nanoparticle assemblies. Langmuir 28(33): 12304–12310.

Parkinson BA, Anson FC (1978) Adsorption and Polymeric Film Formation at Mercury-Electrodes by Solutions of Lead (II) and Chelating Ligands Containing a Thioether Group. Anal. Chem. 50, 1886.

Pierson JF, Wang Y, Ghanbaja J, Soldera F, Boulet P, Horwat D, Mücklich F (2014) Controlling the preferred orientation in sputter-deposited Cu_2O thin films: Influence of

the initial growth stage and homoepitaxial growth mechanism. Acta Materialia 76: 207–212.

Qiao Z, Yang G, Wang J, Li J, He S (2014) Facile synthesis and lithium storage performance of hollow CuO microspheres. Materials Letters, 129: 5–7.
Ryu H, Kim TG, Oh H, Lee WJ (2014) The study of post annealing effect on Cu_2O thinfilms by electrochemical deposition for photoelectrochemical applications. Journal of Alloys and Compounds 612: 74–79.

Sathyamoorthy R, Mageshwari K (2013) Physical properties of nanocrystalline CuO thin films prepared with the SILAR method. Materials Science in Semiconductor Processing 16: 337–343.

Sathyamoorthy R, Mageshwari K (2013) Physical properties of nanocrystalline CuO thin films prepared by the SILAR method. Materials Science in Semiconductor Processing 16: 337–343.

Sato M, Honda T, Takano I, Mochizuki C, Hara H, Suzuki T, Nagai H (2012) Chemical fabrication of p-type Cu_2O transparent thin film using molecular precursor method. Materials Chemistry and Physics 137: 252–257.

Sawyer DT, Sobkowiak A, Roberts JL (1995) Electrochemistry for Chemists. John Wiley & Sons: New York, 2nd Ed.

Solmaz R, Döner A, Doğrubaş M, Erdoğan İY, Kardaş G (2016) Enhancement of electrochemical activity of Raney-type NiZn coatings by modifying with PtRu binary deposits, Application for alkaline water electrolysis. International Journal of Hydrogen Energy 41(3): 1432–1440.

Stoppato A (2008) Life cycle assessment of photovoltaic electricity generation. Energy 33(2): 224–232.

Sze SM, Ng KK (2007) Physics of Semiconductor Devices. John Wiley Sons, New York, 3rd Ed.

URL-1,http://www.bayar.edu.tr/besergil/eak_2_1_referans.pdf (date of access: 2017).

URL-2,http://akademi.itu.edu.tr/dokenb/DosyaGetir/58255/ANL1.pdf (date of access: 2017).

URL-3,abs.mehmetakif.edu.tr/upload/1127_904_dosya.pdf (date of access: 2017).

URL-4, http://www.uksaf.org/tech/edx.html (date of access: 2017).

Wang CW, Zhang XQ, Chen JB, Zhu WD, Liao AZ (2014) Vertically aligned single-crystalline ultra-thin CuO nanosheets: Low-temperature fabrication, growth mechanism, and excellent field emission. Journal of Alloys and Compounds 609: 253–261.

Wang Y, Jiang T, Meng D, Wu X, Wang J, Chen J (2014) Controllable fabrication of CuO nanostructure by hydrothermal method and its properties. Applied Surface Science 311: 602–608.

Wang J (2001) Analytical Electrochemistry, Wiley-VCH, New York, 2nd Ed.

Wijesundera RP, Hidaka M, Koga K, Sakai M, Siripala W (2006) Growth and characterisation of potentiostatically electrodeposited Cu_2O and Cu thin films. Thin Solid Films 500: 241–246.

Yu Y, Aref AA, Xiong L, Yan N, Abdulkarem AM (2011) Cu_2O nanorod thin films prepared by CBD method with CTAB: Substrate effect,deposition mechanism and photoelectrochemical properties. Materials Chemistry and Physics 127: 433–439.

Zhang J, Zhu H, Li C, Pan F, Wang T, Huang B (2009) Cu_2O thin films deposited by reactive direct current magnetron sputtering. Thin Solid Films 517: 5700–5704.

Zhang L, McMillon L, McNatt J (2013) Gas-dependent bandgap and electrical conductivity of Cu_2O thin films. Solar Energy Materials and Solar Cells 108: 230–234.

Zhu W, Liu X, Liu H, Tong D, Yang J, Peng J (2010) Coaxial heterogeneous structure of TiO_2 nanotube arrays with CdS as a superthin coating synthesized via modified electrochemical satomic layer deposition. Journal of the American Chemical Society 132(36): 12619–12626.

CURRICULUM VITAE

In 1982, I was born in Iraq/Erbil. I completed primary and secondary school in Erbil. And then, in 2009-2010, I graduated in Salahaddin University/college of science/chemistry department, successfully. In addition, after four years, I hold the bachelor's certification in that field, approximately, one year after of my graduation. I started to work as assistance chemist in Medical Institute of Polytechnic University in Iraq/Erbil. Furthermore, in October of 2015, I started the study of master degree in Chemistry Department/Analytical Chemistry, Institute of Science, Bingöl University/Turkey.

SHVAN JAWHAR TAHER
Shvanjawhar82@gmail.com
Mob.no:(009647504882939
+9647824082939)